An optical study of stars and dust in the Andromeda galaxy

Walterbos, R.A.M.; Kennicutt jr., R.C.

Astron. Astrophys. 198, 61–86 (1988)

ASTRONOMY AND ASTROPHYSICS

An optical study of stars and dust in the Andromeda galaxy

R.A.M. Walterbos [1,2,*] **and R.C. Kennicutt, Jr.** [3]

[1] Leiden Observatory, P.O. Box 9513, NL-2300 RA Leiden, The Netherlands
[2] The Institute for Advanced Study, School of Natural Sciences, Princeton, NJ 08540, USA
[3] University of Minnesota, Department of Astronomy, 116 Church Street S.E., Minneapolis, MN 55455, USA

Received October 19, accepted December 30, 1987

Summary. We have analyzed the light distribution of the nearby spiral M31, using recently obtained surface photometry in four colours. Three main topics are discussed. First, we study the structure in the outer parts of the disk. Our data confirm previously presented evidence for a significant change in the position angle of the light distribution, probably indicating a warping of the stellar disk. The warping starts at 18 kpc and is in the same direction as the warp in the gas distribution. Second, we discuss the structure and global color distribution of the disk and bulge of M31. A decomposition of the major and minor axis profiles allows us to separate radial color variations in bulge and disk. No color gradient is found for the bulge light. We show that the apparent flattening of the light profile of the disk noted by de Vaucouleurs can be attributed to the contribution from spiral arms. The disk colors at small radii and the colors of the bulge are typically those of an old, metal-rich stellar population. The disk light, corrected for the contribution of spiral arms, becomes bluer with radius, due to a metal abundance gradient or to a contribution from younger stars inbetween the arms. Finally, we derive the optical extinction law in M31 from a detailed analysis of the absorption of light in two major dust lanes on the near side of the galaxy. A correlation of the optical extinctions with neutral atomic gas column densities shows that the dust-to-(atomic) hydrogen gas ratio is similar to that in the solar neighborhood, but may well decrease with radius.

Key words: galaxies: M31 – stellar content of – structure of – dust – extinction – photometry

1. Introduction

In recent years much information has been obtained on the structure and stellar content of spiral galaxies from detailed multicolor surface photometry (e.g. Schweizer, 1976; Talbot et al., 1979; Wevers et al., 1986). Data on the light distribution in galaxies can also be used to analyze the structure and the extinction properties of dust lanes (e.g. van Houten, 1961; Elmegreen, 1980). Until recently, such optical data were lacking for the spiral that is closest to us, the Andromeda galaxy (M31). Ironically, this was due to the fact that the galaxy is too nearby: the angular size is so large that surface photometry of the whole object was an almost hopeless enterprise. Recent advancements in plate scanning devices and computers have made it possible, however, to obtain data on the light and color distribution across the galaxy that are of a quality comparable to that of the material for other spirals. Hodge and Kennicutt (1982) mapped M31 in blue light and Walterbos and Kennicutt (1987, Paper I from now on) extended that work to full two-dimensional photometry in four colors, *U*, *B*, *V*, and *R*.

In this paper we analyze the optical data that were presented in Paper I, focussing on three main issues. In Sect. 3 we discuss the structure of the outer disk of M31 and the decomposition of the light profile in bulge and disk components. In Sect. 4 we analyze the global color distribution across the galaxy, in particular the radial color dependence of the bulge and of the disk. The close distance of M31 (690 kpc) allows us to measure the extinction in some of the major dust lanes and to study the correlation of the optical extinctions with neutral hydrogen gas column densities, obtained from high resolution radio observations. The major part of this paper, Sect. 5, is concerned with this analysis. First, however, we will briefly summarize the data in Sect. 2.

2. Data

Some 15 calibrated plates of M31 in Johnson *U*, *B*, *V* colors, and a photographic *R* band were obtained with the Burrell Schmidt telescope on Kitt Peak and digitized with the Astroscan reticon densitometer at Leiden Observatory. In addition, exposures on IIIaJ and IIIaF emulsions were obtained; these are referred to as *J* and *F*. We combined long and short exposures to cover a large range in surface brightness. The sky background on each plate was subtracted by a modified polynomial fit. After subtraction of the sky background the rms residual intensities in regions where the sky fit was defined were 1 to $1\frac{1}{2}$% of sky, depending on the emulsion type. The final net calibrated intensities have typical uncertainties varying from 0.05 mag at bright levels to 0.2 mag at 3 to 4 mag arcsec^{-2} below sky intensity. Reliable colors (uncertainties less than 0.1 to 0.2 mag) were obtained over the main part of the disk, out to a *B* surface brightness of 24.0 mag arcsec^{-2}, corresponding to a radius of 14 kpc.

The data were recorded at a pixel size of $40 \times 40\,\mu m^2$ (3.864×3.864 arcsec^2), but the maps used for the analysis in this paper were compressed versions with pixels of $160 \times 160\,\mu m^2$

Send offprint requests to: R. Walterbos (California address)

* Present address: Astronomy Department, University of California, Berkeley, CA 94720, USA

corresponding to an angular size of 15.456×15.456 arcsec^2 or a linear size of 50×50 pc^2. In each color, three maps were available, one with foreground stars still present, one from which the brightest stars were removed, and one from which essentially all foreground stars were removed with a "rigorous star removal" routine. The method used to remove the stars is described in Paper I. In the last set, some of the high resolution structure of the galaxy is lost due to the automated nature of the method. This does not affect global quantities, however, and all radial distributions presented in this paper were obtained from the maps to which the rigorous star removal routine was applied. In the study of the dust lanes in Sect. 5 the maps from which only the brightest stars were removed were used; on these maps the high resolution structure associated with the galaxy is not affected.

3. The structure of the stellar disk and bulge

3.1. The outer regions of the disk

The deep J image presented in Paper I showed a clear change of the position angles of the isophotes on the southern major axis for radii larger than 90′, suggesting a warping of the stellar disk. Innanen et al. (1982) found similar results from digital stacking of plates in several colors. Baade (1963) mentioned that the Population II stars seem to "swirl off" to one side, on both sides of the major axis. From Baade's discussion it is not clear in what direction he saw a displacement. Warped stellar disks have been found in some edge-on galaxies, for example in NGC 4565 (van der Kruit and Searle, 1981; Jensen and Thuan, 1982).

Our material allows an independent study of the outer regions, including a better estimate of the surface brightness levels at which a potential warp occurs, because the data are calibrated. We stacked two sets of plates, one set consisting of two long exposures in R and two long exposures in F, the other set of two long B and two long J exposures. The resulting images are displayed in Fig. 1, at maximum contrast to show the faint emission. On the southern side the change in position angle at the outer edges is very convincing and the structure suggests that the displaced emission is associated with M 31. A twisting of the isophotes in galaxies that are not completely edge-on, may also result from spiral arms that "open up" in the outer part of the disk. This is for instance the case in the spiral NGC 4258 (Van der Kruit, 1979). The isophotes in the outer regions of M 31 (Paper I), do not show the kind of structure that is observed in NGC 4258 where steep gradients, associated with the outer edge of the spiral arm, are present; nevertheless it is difficult to rule out completely that the observed structure is actually due to spiral arms. We will continue to use the term "warp" here though, for consistency with earlier discussions. The warping on the South side starts below a B-surface brightness of 25.0 mag arcsec^{-2} and below about 23.6 mag arcsec^{-2} in R. Our data are not accurate enough to obtain reliable colors for individual regions at these levels. The global light profile, integrated over azimuthal angle (Paper I) indicates a $B-R$ for the outer regions of about 1.3 mag.

For the northern half the evidence for a warp is not as strong. Faint light bending away from the northern major axis is present on our red and blue images, but it is not completely obvious that it is associated with M 31. The differences in structure and intensity of the diffuse emission for the two halves of the galaxy are also evident in the images of Innanen et al. (1982). The faint emission could be due to a galactic reflection nebula; the ubiquitous presence of such material has recently been established by infrared (e.g. Low et al., 1984) and optical observations (de Vries and Le Poole, 1985). If the diffuse light on the northern half is due to a real warp, it would probably be the most extreme warp in a stellar disk ever found so far.

A possible disagreement with Baade's (1963) findings concerns the position at which the warp starts. Baade states that this occurs at a distance of two degrees, while our images and those from Innanen et al. (1982) show the twisting of the isophotes to start at 1.5 to 1.7 degrees on both halves. The warp in the H I gas on the major axis seems to begin at about 2 degrees (e.g. Newton and Emerson, 1977; Cram et al., 1980). Models of the warp, based on analysis of complete H I data sets, however, indicate that the warping begins at about 1.3 degrees from the center (Henderson, 1979; Brinks and Burton, 1984). The orientation of the H I warp agrees with the direction of the twist of the optical isophotes, but, apparently different from the situation in the optical, the warp angle of the H I on the major axis is small, and the maximum warping occurs almost on the minor axis (the line of nodes of the H I warp differs only 20 degrees from the line of nodes of the disk; Brinks and Burton, 1984). Evidently, a new study of the structure of the disk and of the stellar population in the disk at large radii in M 31 would be most useful.

3.2. Decomposition into bulge and disk

Bulges of spiral galaxies have a light profile similar to that of elliptical galaxies and can be well fit by a de Vaucouleurs (1948) law:

$$I(r) = I_e \, 10^{-3.33[(r/r_e)^{1/4}-1]}, \quad (1)$$

where r_e is the effective radius within which half of the total light is concentrated, and I_e is the intensity at r_e. Disk profiles can usually be represented by an exponential law (Freeman, 1970):

$$I(r) = I_0 \, e^{-r/r_1}, \quad (2)$$

where r_1 is the exponential scalelength and I_0 the intensity at zero radius. Several galaxies possess structures usually associated with bars, lenses, or regions with strong concentrations of star formation activity, that cannot be represented by these two components (e.g. Boroson, 1981; Kent, 1985). Decomposition of M 31's light profile in disk and bulge components is nevertheless important for comparison of M 31 with other galaxies. In addition, the separation makes it possible to estimate the relative contributions from disk and bulge across the galaxy, and to look for possible radial color gradients in either bulge or disk.

The inclination of M 31 (77°) introduces severe projection effects that are different for bulge and disk, because of the differences in scaleheight of these two components. For this reason the global light profile presented in Paper I could not be used for the decomposition. We compiled average profiles for the two halves of the major axis of M 31 in all four colours ($U\,B\,V\,R$) by averaging the light distribution in circles in the plane of the galaxy (corresponding to ellipses in the sky plane) over a range of 100 degrees in azimuth for each major axis half (cf. Walterbos and Schwering, 1987). The 100 degree cone in the plane of the galaxy corresponds to only 30 degrees in the sky plane; thus the average profile is not strongly influenced by projection effects, but it does have a considerable better signal-to-noise ratio than a direct major axis cut. For the inner $\pm 14'$ we did use the directly observed intensities on the major axis, because the azimuthally averaged values were about 10% too bright in this region; this is due to the thickness of the bulge. This point was not recognized in an earlier

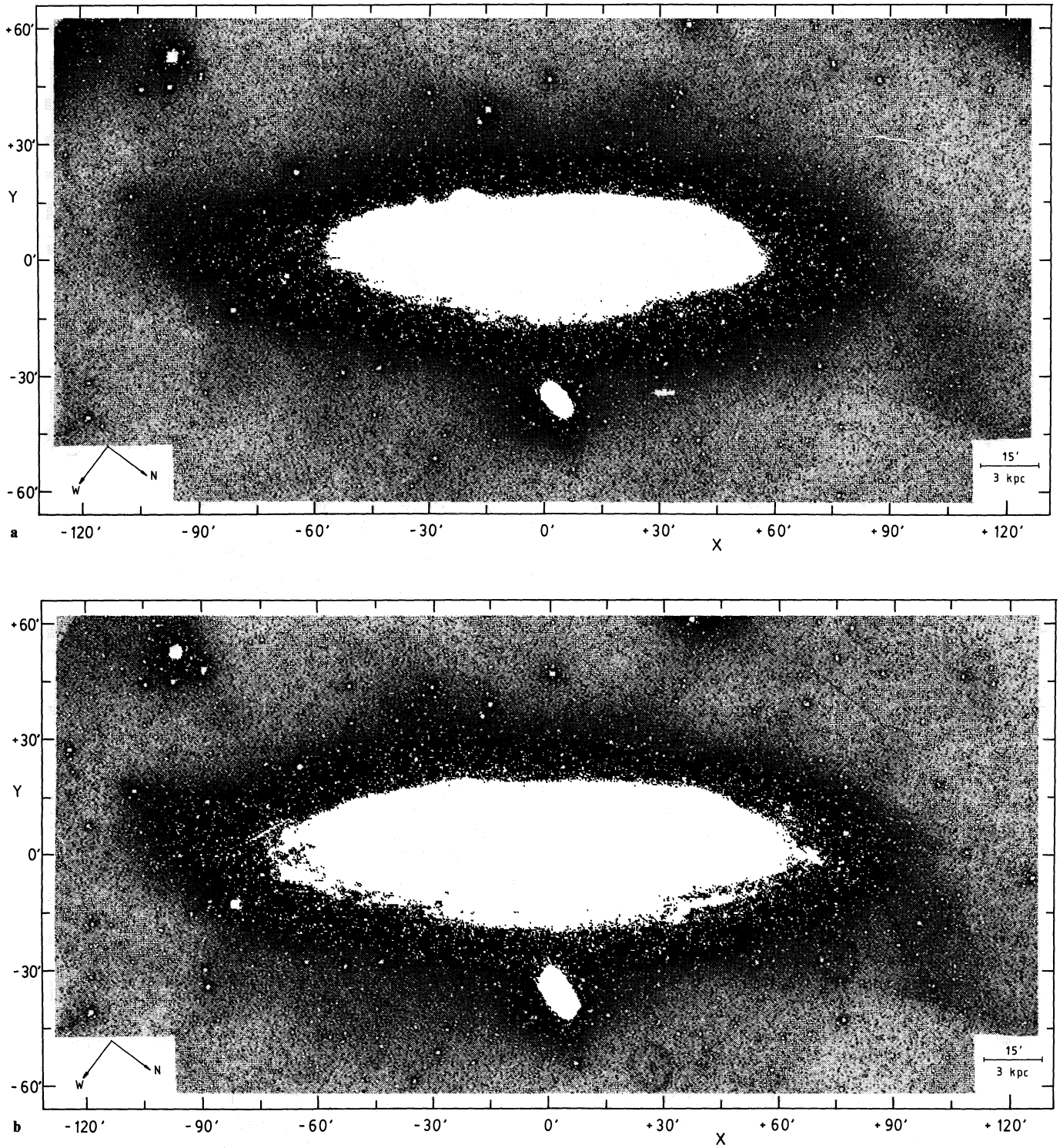

Fig. 1a and b. Deep red (**a**) and blue (**b**) images obtained by stacking calibrated images of four plates in each color. The grey scale is chosen in such a way that maximum contrast at low light levels is achieved. The strong change in p.a. of the light distribution on the Southern major axis near $X = -100'$ suggests a warping of the stellar disk. In the Northern part diffuse light bending away from the major axis is present in both colors, but the association with M 31 is less convincing than in the South. Ghost images of stars are visible in **b**, e.g. near $(+28', -50')$ and $(+75', -25')$. The narrow spikes in **b** are caused by the bright star ν And located at $(+40', +65')$

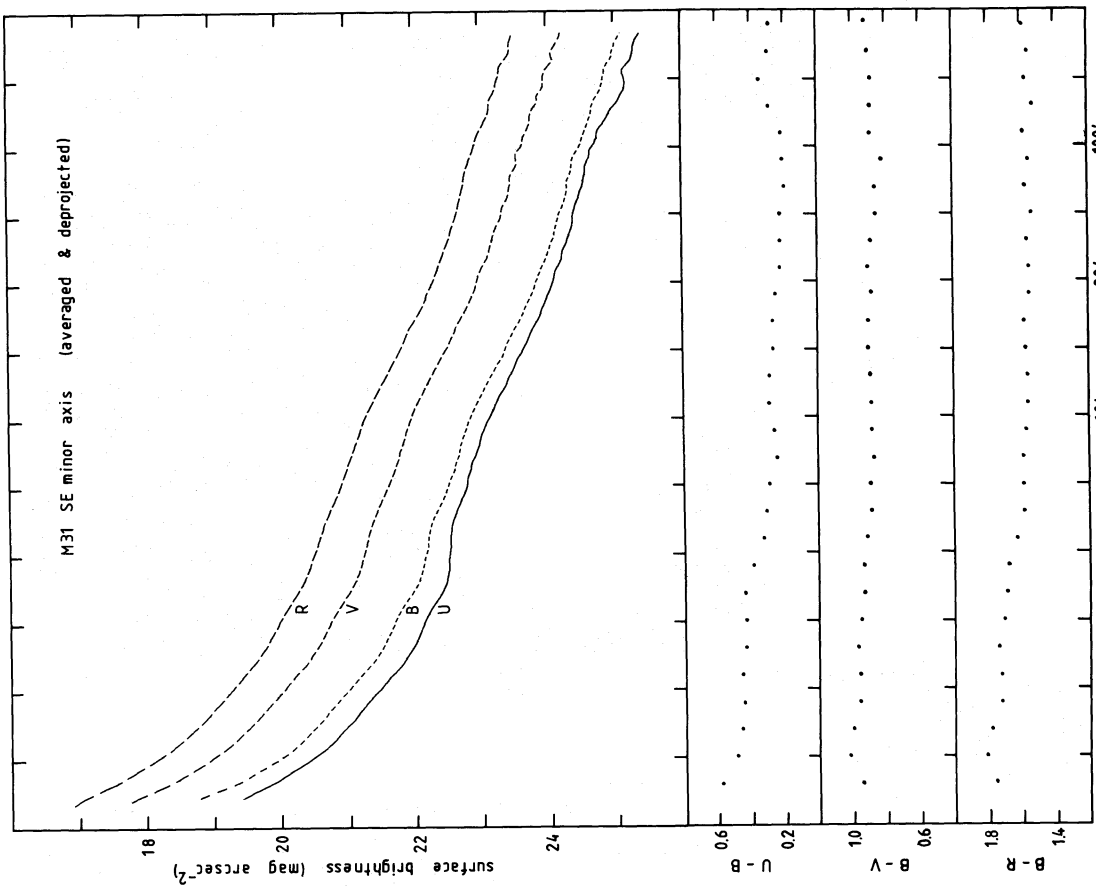

Fig. 2a. Azimuthally averaged intensity and color profiles for the SW and NE parts of the major axis of M31. Foreground stars were removed from the maps beforehand. The photometric uncertainties increase rapidly for radii greater than 80′ to 90′. The profiles for the SW half are shifted upwards by 3 mag for clarity. The data are not corrected for foreground reddening

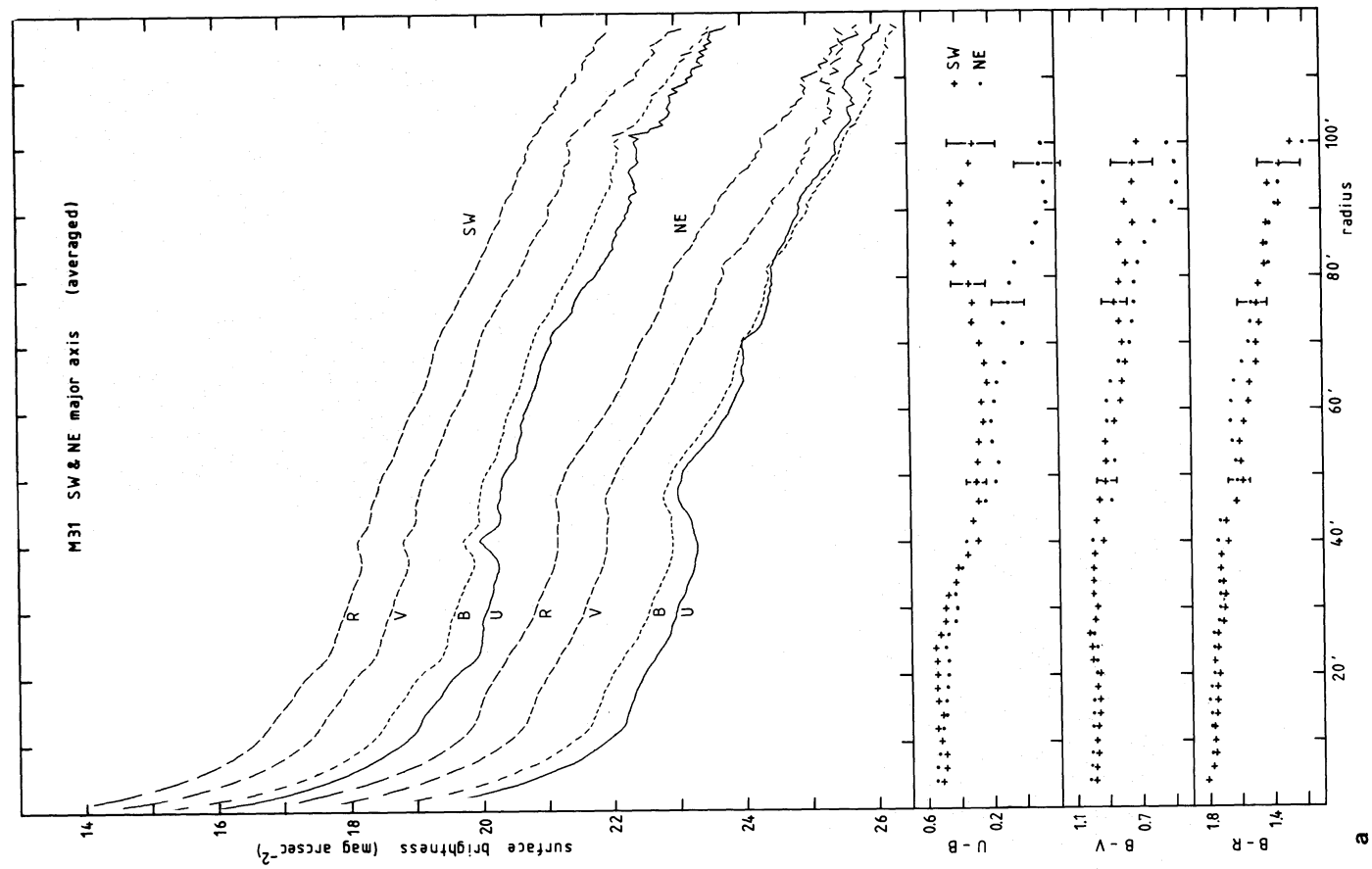

Fig. 2b. Azimuthally averaged intensity and color profiles for the far (SE) minor axis side of M31. Notice that the radial color variation is less here than for the major axis; this is due to the large contribution to the intensities from the bulge on the minor axis (Fig. 3b). The horizontal scale has been expanded by $1/\cos(i)$ to obtain a face-on projection. The colors are not corrected for foreground reddening

discussion of the light profile (Walterbos, 1986). As a result, the disk and bulge parameters presented here are slightly different. Similarly, a minor axis profile was derived by averaging the light distribution in circles on the plane of the galaxy over 20 degrees in azimuth around the minor axis. Only the data for the far side of the galaxy were used, because the near side is severely influenced by obscuring dust (Sect. 5). Maps to which "rigorous star removal" had been applied (Paper I) were used. The intensity profiles are shown in Figs. 2a and 2b.

Upon first inspection, the profiles do not exactly match the sum of an $r^{1/4}$-law bulge and an exponential disk. The SW major-axis profile shows a distinct peak at 40′ that is due to NGC 206, the brightest OB association. The broad plateau following this peak, extending from 45 to 80′, coincides with the region where major spiral arms are present; the arms overlap in the average profile, resulting in one broad hump. An outlying spiral arm can be seen around 100′. On the NE side the arms are better separated. Especially the arm corresponding to the 10 kpc "ring" at 50′, where most of the Population I material is concentrated, is apparent. In contrast to some of the spirals studied by Schweizer (1976) and Wevers (1984), M 31 does not seem to show an increase in the arm-to-disk ratio with increasing radius. That we are seeing the contribution from spiral arms is also indicated by the asymmetry between NE and SW halves, and by the color changes in these regions. Note that this does *not* imply that all excess light is due to young stars; a significant part of the light from spiral arms stems from evolved stars (e.g. Schweizer, 1976; Kennicutt and Edgar, 1986). In any case, it appears that the hump in the profile around 50′ does not reflect the global disk structure, but is due to the contribution from spiral arms. Freeman (1970) classified the light profile of M 31 as type II, because of this hump. The disk fits to type-II profiles are generally too bright in the inner region which implies that there would have to be a "hole" in the real disk. In view of the discussion above, it is more likely to assume that there is excess light, associated with the spiral arms, on top of the disk of M 31 instead of a hole in the center. In a similar way, Talbot et al. (1979) showed that the flattening of the light profile of M 83, another proto-type II, was due to the contribution from relatively blue regions.

We fitted the sum of an $r^{1/4}$ law and an exponential disk to those regions of the profiles that were not influenced by spiral arm structure. From the profiles in Fig. 2a it is clear that it is difficult to unambiguously identify these regions at large radii. Nevertheless, by using the same regions for all colors a good impression of the underlying disk can be obtained. For the inner 5′ our data were complemented with CCD photometry by Kent (1983). The two major-axis profiles were used together to define initial disk and bulge parameters. The resulting fit was then applied to the minor-axis profile, with only the axial ratio of the bulge as a free parameter. An inclination of 77° was assumed. The process was iterated a few times to obtain the most satisfactory fit to all profiles. We did not attempt to fit regions beyond 100′, because the photometric errors increase rapidly at larger radii. Points inside 1.′5 were excluded because the central core of M 31 cannot be fit by an $r^{1/4}$ law (Kent, 1983). The resulting fit to the B profiles is shown in Fig. 3a for the major axis and Fig. 3b for the minor axis. The parameters of the fits are listed in Table 1. The residuals, displayed in the lower part of the figure, indicate an average arm-to-disk ratio in B of 20 to 50% for the major spiral arms. This is similar to the results found for some other spirals, (e.g. Schweizer, 1976; Kennicutt and Edgar, 1986). Around 20′ some excess light seems to be present that cannot be represented by the sum of an exponential and an $r^{1/4}$ law. This hump is more clearly visible in the direct major axis profile (Paper I); it may indicate the presence of a weak lens component, or perhaps an inner spiral arm. All major-axis profiles decline more rapidly beyond 90′ than the exponential fits; this is perhaps related to the warping of the disk. However, as mentioned before, the uncertainties are large here (>0.2 to 0.3 mag) and more accurate photometry is needed to settle that point. The spiral arm structure corresponding to the ring around 10 kpc is also visible in the minor axis profile, as is clear from the residuals in Fig. 3b.

The bulge profile is reasonably well represented by an $r^{1/4}$ law. The fit indicates an apparent axial ratio of 0.65 for the bulge, corresponding to a true axial ratio of 0.63 or a z-height of 1.25 kpc (for an oblate spheroid). The central region of the bulge is somewhat less flattened (Kent, 1983), which explains the positive residuals between 2′ and 5′ in Fig. 3b. The actual three-dimensional structure is more complicated than an oblate spheroid. The position angle of the bulge changes more or less continuously (e.g. Hodge and Kennicutt, 1982; Kent, 1983; cf. Fig. 4 in Paper I), indicating that the bulge is triaxial or perhaps contains a bar (Lindblad, 1956). The change in position angle for the bulge is not taken into account in a decomposition of major- and minor-axis profiles; this may have resulted in a slight underestimate ($\sim 10\%$) of the effective radius of the bulge.

Our decomposition is different from that presented by de Vaucouleurs (1958) who, on the basis of the apparently flat disk profile, subtracted a constant disk surface brightness inside 50′ radius and then fitted an $r^{1/4}$ law to the bulge. The effective radius that we derive, 2.0 kpc, is smaller than that found by de Vaucouleurs, 3.5 kpc, the intensity at the effective radius higher, 22.2 compared to 22.9 mag arcsec^{-2}. Ciardullo et al. (1987) also discussed the decomposition of M 31's light profile and found the same bulge parameters as de Vaucouleurs. The different result is probably due to two reasons. First, Ciardullo et al. basically used the same data as de Vaucouleurs. They also included Kent's (1983) photometry, but that only covers the very inner region where the $r^{1/4}$ law is not followed very well (Fig. 3a). The photometry for regions brighter than $B = 21.80$ mag arcsec^{-2} was not directly observed by de Vaucouleurs, but obtained by correcting data from other sources, dating back as far as 1934. It is quite likely that the data in this region, which is crucial in defining the bulge characteristics, are less reliable than the more recent photometry by various authors, discussed in Paper I. Second, Ciardullo et al. did not exclude the inner 1.′5 from the fit; this results in a flatter bulge profile. The difference between their and our decomposition can be assessed from comparing Figs. 4a and 4b, where we show the fit they propose, with Figs. 3a and 3b. The difference in the residuals is not that dramatic, which illustrates the difficulty of performing unambiguous bulge-disk decompositions, even in relatively well-measured galaxies. This is in particular true for the effective radius in the $r^{1/4}$ law. Nevertheless, comparison of Figs. 4 and 3 does suggest that our decomposition is somewhat more consistent with the data. In particular, the large effective radius for the bulge is not supported by the minor axis profile and the bulge fit proposed by Ciardullo et al. seems to be too bright around 10′ on the major axis.

The integrated intensity for the bulge is derived from the fit:

$$I_{\rm int} = 7.215\pi\, I_e r_e^2 \frac{b}{a} \qquad (3)$$

(e.g. de Vaucouleurs, 1958), where b/a is the apparent ratio of minor to major axis and the other parameters are as in (1). It is lower than the value from de Vaucouleurs, 5.39 mag in B versus 4.92 mag (The 5.92 listed in his paper should be 4.92). Integrated

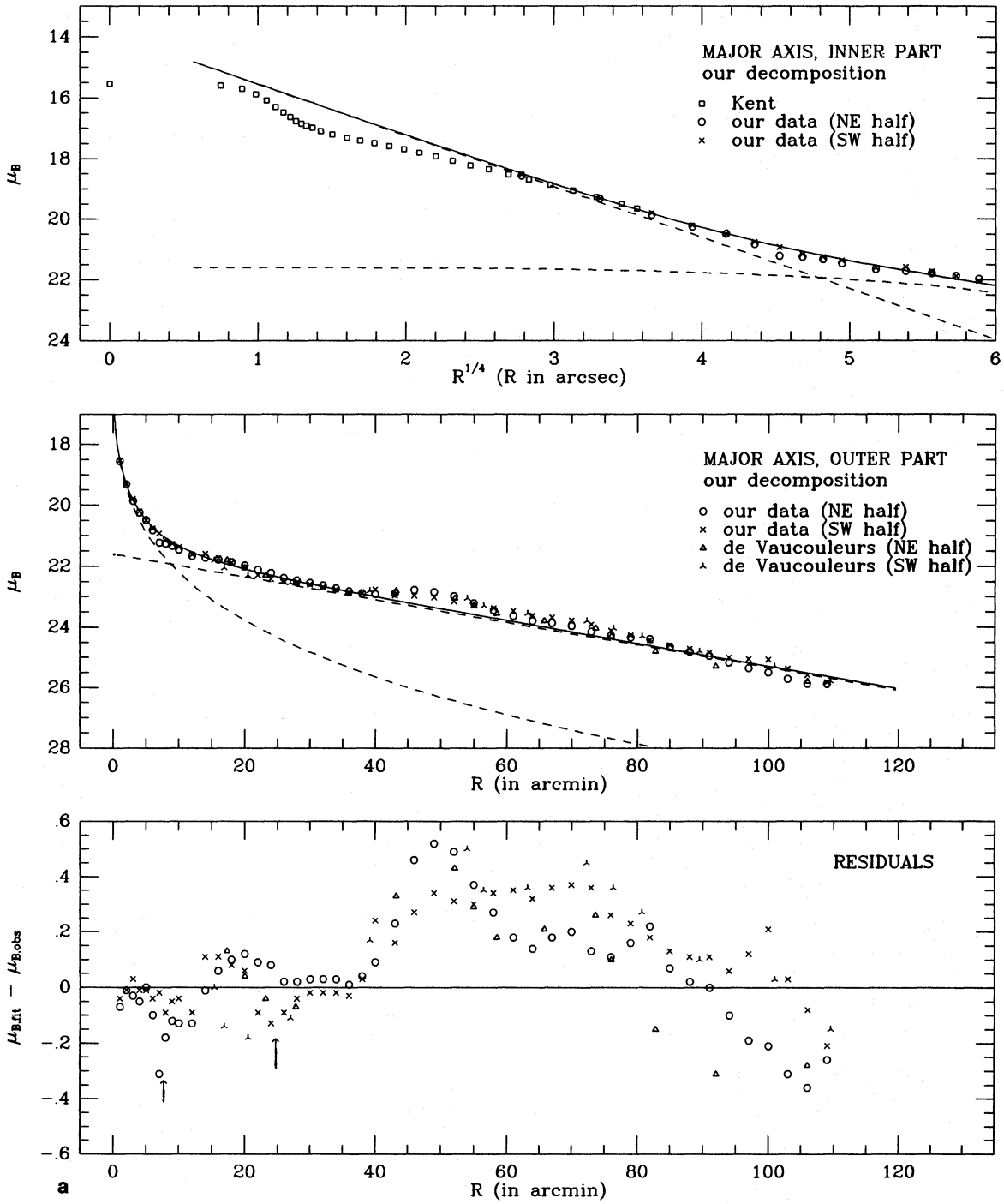

Fig. 3a. The decomposition of the major axis profiles in *B* into bulge and disk components (dashed lines). The full drawn line is the sum of the bulge and disk fit. Regions with spiral arm structure were excluded from the fit. Points at radii larger than 100′ were also not used, because photometric errors are large there. The top panel shows the inner region plotted as a function of $r^{1/4}$. The CCD photometry by Kent (1983) is included; a zero-point offset was applied to his *r*-band data to align them with our *B*-band photometry. The middle panel shows the outer regions. The agreement between the data from de Vaucouleurs (1958) and our measurements is excellent. The residuals are displayed in the bottom panel. The arrows indicate regions where the light distribution is notably influenced by dust. The residual intensities correspond to spiral arms; the hump around 20′ may indicate a lens. The structure on the SW half is abnormally broad, because spiral arms overlap in the average profile

bulge magnitudes in the other colors directly follow from the constant color for the bulge (Sect. 4). Subtracting the bulge magnitudes from the total magnitudes derived in Paper I, gives the integrated disk magnitudes. Notice that these now include the contribution from the spiral arms.

The bulge and disk parameters following from our decomposition are within the range observed for other Sb galaxies (e.g. Boroson, 1981; Kent, 1985). The central surface brightness of the disk has to be corrected to a face-on value for comparison with other galaxies, but this is not straightforward for a galaxy with

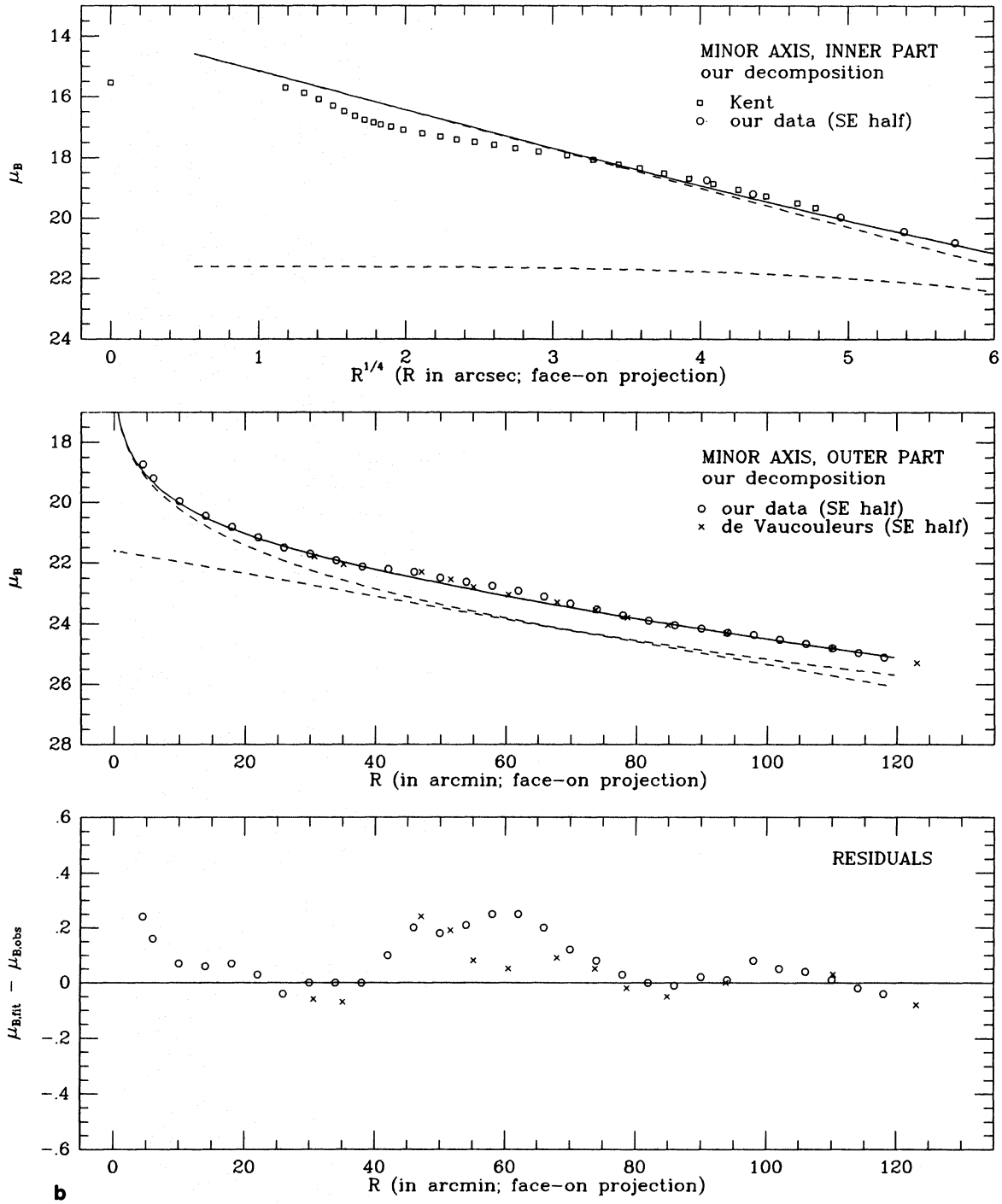

Fig. 3b. The decomposition of the average minor axis profile on the far side of M31. Notice that due to projection effects the bulge is brighter than the disk everywhere. The residuals in the bottom figure again clearly show the region with major spiral arm features between 40′ and 75′

such a high inclination. A purely geometrical correction for the inclination ($-2.5 \log(\cos(i))$ is too strong as it neglects the effects of internal extinction. Kent's (1985) results indicate that, statistically, a correction of $-1.7 \log(\cos(i))$ is a better approximation. If we combine this with the correction for foreground reddening, $A_B = 0.3$ (e.g. van Genderen, 1969; Walterbos and Schwering, 1987), we derive $B_0 = 22.4$ mag arcsec^{-2}. This value is somewhat fainter than the canonical 21.6 mag arcsec^{-2} (Freeman, 1970; Boroson, 1981; Kent, 1985), but similar to that found for some other Sb's, e.g. NGC 7331 (Boroson, 1981). The bulge-to-disk ratios in the various colors are listed in Table 1 as well. The bulge contributes roughly 40% of the total intensity. Note, however, that the values in Table 1 are not corrected for internal extinction, which is likely to be more important in the disk than in the bulge. In comparison with other Sb's (Boroson, 1981; Kent, 1985), M31 has a rather prominent bulge. Van der Kruit (1984) recently compiled data on the bulge (spheroid) and disk of the Milky Way and its morphological twin NGC 891. The size of M31's bulge is of

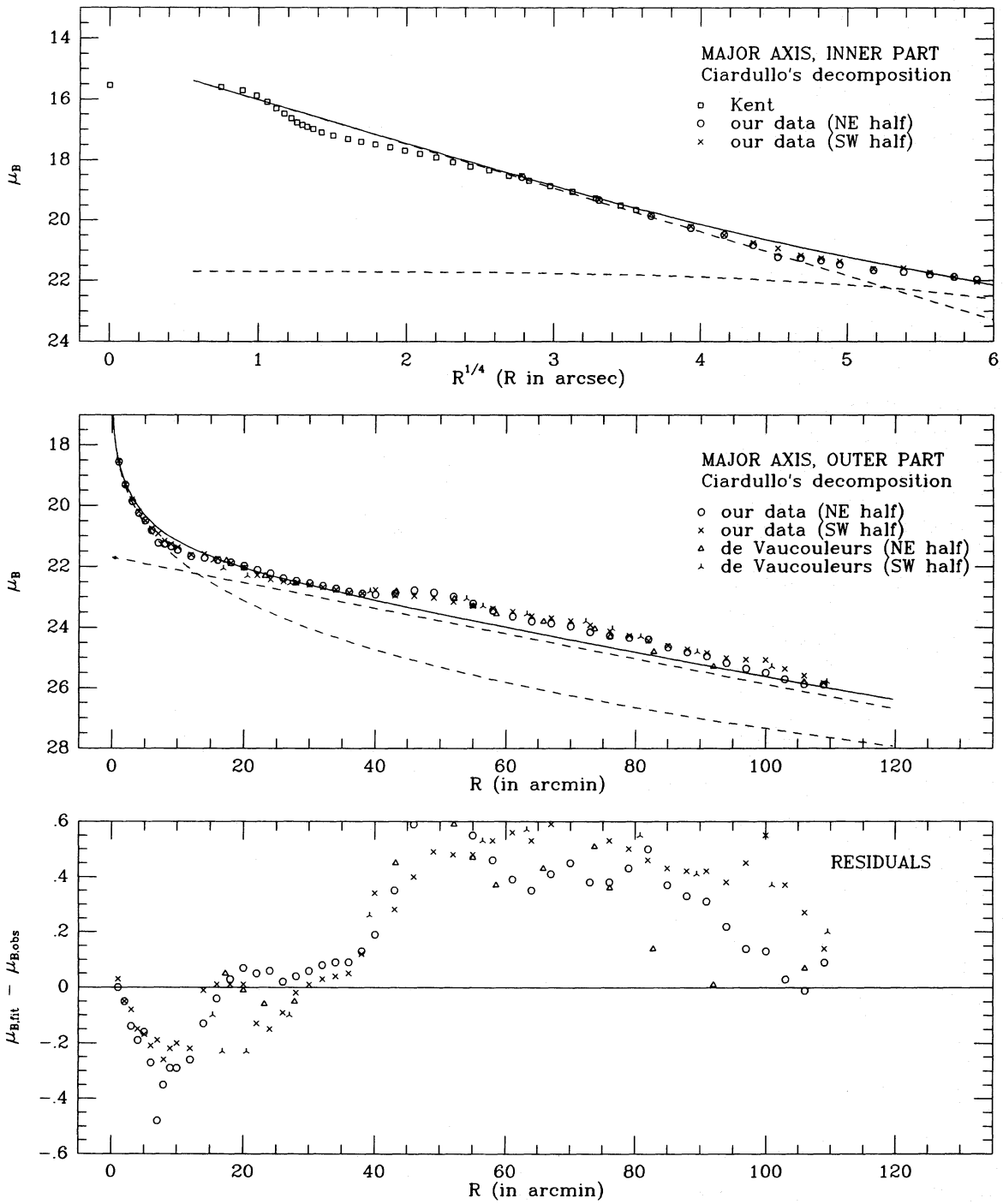

Fig. 4a. The decomposition of the light profile of M 31 on the major axis, proposed by Ciardullo et al. (1987). The major difference with our decomposition is in the bulge fit (effective radius is twice as large here)

the same order as that of these two galaxies, but the total brightness is about a factor of 3 to 4 higher; the disks are quite comparable.

4. The global disk and bulge colors

One of the purposes of the separation of the disk and bulge of M 31 was to look for color gradiens in these components. Radial color variations in the bulge may be expected if a metal abundance gradient, presumably set up during the formation of the spheroidal component of the galaxy, exists. For the disk, color variations reflect metal abundance variations or differences in the age of the stars in the disk. Dust may produce apparent color variations. Observations of color gradients in spiral galaxies so far have not resulted in a clear picture. Evidence for color gradients in bulges comes from photometry of edge-on systems (Van der Kruit and Searle, 1981, 1982b), but the magnitude of the color

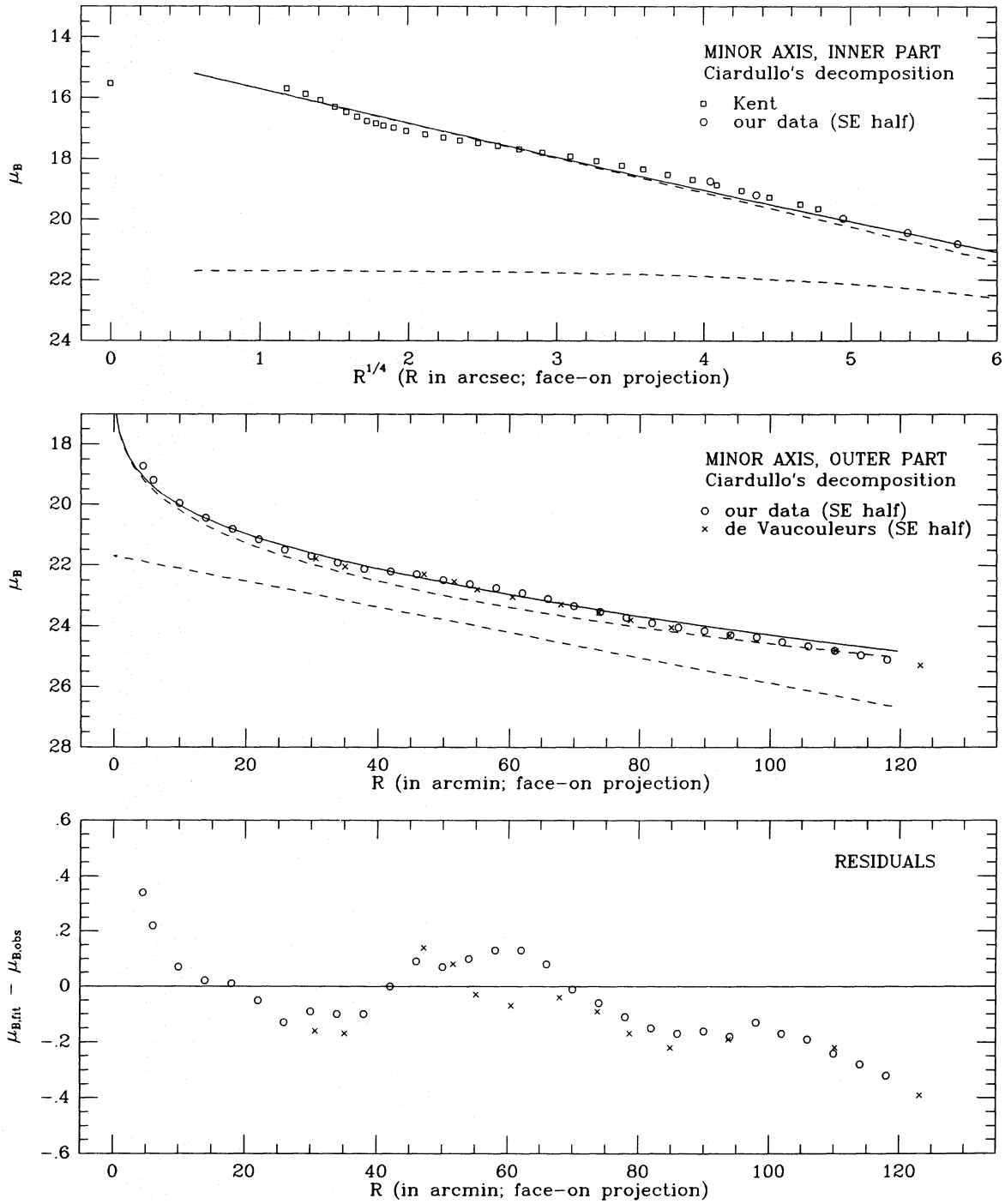

Fig. 4b. Same as Fig. 4a but now for the minor axis. The data in the outer parts do not seem to support the large effective radius for the bulge proposed by Ciardullo et al. (1987)

variations differs from galaxy to galaxy. Color variations in the disk seem to be rather small, especially if the contribution from young stars in the spiral arms is subtracted. Schweizer (1976) found a gradient in the disk colors in only one (M81) out of six galaxies. Jensen et al. (1981) detected a gradient in the inner part of the underlying disk of M83. Van der Kruit and Searle (1981, 1982a) found no significant (< 0.3 mag) radial color variations in the old disks of edge-on systems, at typical distances of 1 kpc above the plane. Wevers (1984), from a study of a large sample of spiral galaxies, did not detect systematic trends in the radial color distributions of the total disk light.

The different contributions of the disk and bulge of M31 on the major and minor axis make it possible to separate color variations in the disk from those in the bulge. Because the disk mainly contributes on the major axis, the color variations there have to be due to the disk. Comparison of Fig. 2a with Fig. 2b shows that the color variations along the major axis are larger than those along the minor axis. Decomposition of the light profiles in

Table 1. Bulge and disk parameters for M31 [a]

Parameter	Value	Remarks
Bulge		
Effective radius, r_e	2.0 kpc	Fit to B profile [b]
True axial ratio	0.63	For oblate spheroid
B intensity at r_e	22.2 mag arcsec^{-2}	
$U-B$	0.50 ± 0.03	Zero point errors not
$B-V$	1.05 ± 0.03	included
$B-R$	1.75 ± 0.03	
Integrated magnitude in B	5.39	From fit
Disk		
Central surface brightness	21.60 B mag arcsec^{-2} ±0.10	Not corrected for inclination
Scalelength		
U	6.8 ± 0.4 kpc	Exponential law,
B	5.8 ± 0.3 kpc	followed out to 18 kpc,
V	5.3 ± 0.3 kpc	corrected for spiral arms
R	5.2 ± 0.3 kpc	
Color in center		Colors of fitted disk
$U-B$	0.55	
$B-V$	1.05	
$B-R$	1.80	
Color at 20 kpc		Colors of fitted disk
$U-B$	0.00	
$B-V$	0.70	
$B-R$	1.37	
Color gradient		
$U-B$	$0.03\ \pm0.01$ mag/kpc	
$B-V$	0.018 ± 0.008 mag/kpc	
$B-R$	0.019 ± 0.008 mag/kpc	
Integrated magnitude		
U	5.22	Total – bulge
B	4.93	
V	4.12	
R	3.40	
Bulge to disk ratios, $L_b/(L_b+L_d)$		Observed values, so no
U	0.35	correction for internal
B	0.39	extinction
V	0.45	
R	0.45	

[a] Colors and intensities are *not* corrected for foreground extinction ($A_B=0.3$) or internal extinction

[b] Errors for the bulge fit parameters are difficult to give, because r_e and B are strongly coupled; if r_e goes down, B at r_e would be higher (see Sect. 3)

all colors showed that the reduced color variation along the minor axis can be explained by the larger contribution from the bulge there, combined with a constant color for the bulge. Thus, the bulge does not show a significant color gradient between 0.5 and 5.0 kpc, the range covered by our data. The $U-B$ color decreases by at most 0.15 mag, and the $B-R$ color by at most 0.1 mag. In this respect M31is different from the edge-on Sb NGC 891 where van der Kruit and Searle (1981) find significant color variation (1.0 to 0.7 in $B-V$, 0.4 to -0.1 in $U-B$). The color of the bulge ($B-V=1.05$, $U-B=0.50$) is typical of that of elliptical galaxies, but redder than that of most globular clusters in M31 (e.g. Elson and Walterbos, 1988).

The scalelengths of the disk fits (Table 1), show that there is a radial color gradient in the disk. The variation is not large, but probably real because it is consistently present in all colors. As a result of the difficulty in selecting regions not contaminated by spiral arms in the outer parts of the disk, the gradients listed in Table 1 are probably upper limits; some contamination from spiral-arm light may be present at large radii. The color variation is very similar to that observed in the inner 3 kpc of the old disk of M83 by Jensen et al. (1981). It is unlikely that extinction by dust causes the gradient, because the reddening free index Q, defined as $(U-B)-0.72(B-V)$ (not shown here) also shows a color variation. In addition, for a normal reddening law, extinction

would not result in a color difference larger in $U-B$ than in $B-V$ (cf. Sect. 5). The central colors of M31's disk, ($U-B=0.50$, $B-V=0.95$, after correction for foreground extinction) are typically those of an old, metal-rich stellar population; the equivalent spectral type is G5, III or K0, V.

Most if not all of the color gradient in the disk can be accounted for by a radial abundance gradient in M31. The stellar population models of Tinsley (1980) indicate that a metallicity gradient of a factor of 5–10 between 0–20 kpc would reproduce the observed color gradients, and measurements of the interstellar gas abundances by Blair et al. (1982) show an actual gradient of a factor of 5 over this range. It is also possible that a part of the color gradient reflects a change in the mean age of the stellar population with radius, but this effect should be small, because the spiral arm regions were excluded from the fit.

5. Dust and gas in two spiral arms

5.1. Optical extinction and reddening law

Dust lanes and dust clouds in M31 are very conspicuous in optical pictures of the galaxy, but in spite of the clear appearance only limited information on their extinction properties is available. Baade (1963) used the dust lanes as tracers of spiral arm structure in the inner parts of the galaxy. Hodge (1980) presented a catalog with the positions and sizes of some 700 dust clouds. Hodge and Kennicutt (1982) estimated the extinction in a few isolated dust clouds from surface photometry in the blue. The extinction in the dust lanes along the minor axis was studied by Hoessel and Melnick (1980) and by Hodge and Kennicutt (1982). Gallagher and Hunter (1981) analyzed compact dust clouds in the central region. Other information on the extinction properties of the dust in M31 comes from studies of individual objects, such as Cepheids (Van Genderen, 1973) or globular clusters (e.g. Iye and Richter, 1985 and references therein).

We will analyze the properties of the dust in M31 in considerable detail below. However, some information on the extinction law follows directly from Fig. 5 where we show a $U-V$ color image of the inner part of the disk (out to 12 kpc) and a map of the color index Q, defined as $(U-B)-0.72\,(B-V)$. The Q index is reddening free if the dust is in front of the light and if it follows the same extinction law as in our Galaxy. Dust lanes appear as dark bands in the $U-V$ image and are especially well visible on the near (West) side of M31. The light colored regions correspond to young stars in the spiral arms; these are strongly concentrated in the ring at 10 kpc. The remarkable thing is that the dust lanes are completely absent in the map of the reddening free index. This immediately suggests that the reddening law in M31 will not be very different from that in the Milky Way. The significance of this result can be assessed from the analysis presented below. The uniformity of the Q color in the part of the disk interior to the 10 kpc ring indicates that the paucity of star formation regions there, as indicated by optical surveys of the OB associations (van den Bergh, 1964) and the H II regions (Baade and Arp, 1964; Pellet et al., 1978), is a real effect and not due to dust obscuration.

5.1.1. Method of analysis

Analysis of the extinction in the dust lanes in external galaxies from multi-color surface photometry is difficult because of lack of knowledge of the geometry of dust and light sources, of the true intensities, and of the absorption and scattering properties of the dust grains. Detailed studies with a complete treatment of the radiative transfer in the clouds, including the effects of scattering, have been presented by for example van Houten (1961) and Elmegreen (1980); these authors clearly demonstrate the complexities that are involved and the large number of assumptions that have to be made. Van Houten's study in particular shows that one cannot hope to learn much about the physical properties of individual dust grains from broadband photometric studies.

We adopt a much more simple approach, which nevertheless provides useful information on the global properties of the dust, such as the extinction law and the relation between dust and H I gas. The high inclination of M31 hampers most observational studies, but in the case of the dust lanes it helps, because to first order the dust on the near side of the galaxy is in front of the light of the galaxy, while the far side of the galaxy can be assumed to be unobscured. The situation is sketched in Fig. 6. Not only the bulge is behind the dust lanes on the near side, but also most of the disk light. Because of the thickness of the disk in combination with the exponential decrease of the intensity with radius, the disk light behind the dust on the near side stems from relatively smaller radii than the disk light behind the dust on the far side. We assume that the light distribution of the galaxy is point-symmetrical with respect to the nucleus and define the observed extinction on the near side at wavelength λ, A_λ, by

$$A_\lambda \equiv -2.5 \log \left(\frac{I_{\text{near}}}{I_{\text{far}}}\right). \tag{4}$$

The symmetry argument has been used before in studies of spiral galaxies (e.g. Lindblad, 1941; Elvius, 1956) and the term "light asymmetry" was sometimes used to denote A_λ. The assumption of symmetry with respect to the nucleus may not be true for the disk if spiral arms are present. This is particularly so for the U intensities, which are most affected by OB associations in the spiral arms. Usually, the associations can be identified on the multi-color scans and no serious errors are introduced. The extinctions derived in this way are lower limits to the true extinction for several reasons:

1. The dust is not completely in front of all the light. The effects of this are analyzed below.

2. The neglect of light scattering. In general, part of the light from directions other than the line of sight, is scattered into the line of sight, resulting in a higher intensity towards the dust lanes than should have been observed.

3. The assumption that the far side is not obscured is not quite true. However, if more than 80% of the light is in front of the dust on the far side, which is quite likely, the maximum observed extinction cannot be more than 0.25 mag. The observed extinctions in the dust lanes that could be traced on the far side were always less than this.

We now first establish the relation between observed and true extinctions if some of the light is in front of the dust. Two extreme cases are considered, viz. an infinitely thin dust layer with an optical thickness τ_V, situated somewhere in a stellar disk (e.g. Elvius, 1956; Gallagher and Hunter, 1981; Price and Grasdalen, 1983), and a uniform mixture of stars and dust. Scattered light is not treated in this analysis, but it is assumed that both the absorbed and the scattered light in the layer never reach the observer, in other words we consider "pure" extinction. The possible influence of light from the bulge that is scattered off the dust in the disk in the direction of the observer will be discussed later.

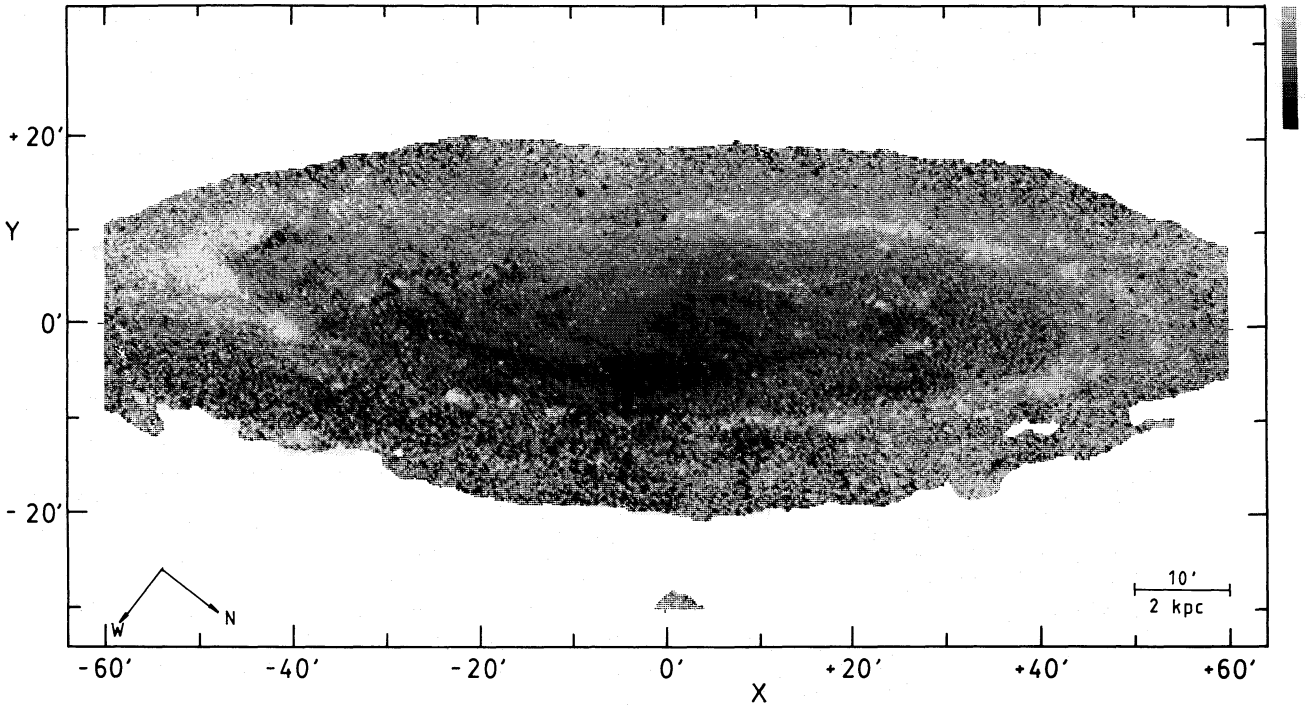

Fig. 5a. High resolution (15″ square pixels) $U-V$ color image of M31. Red regions, such as dust lanes are relatively dark; blue regions appear light. The region around 10 kpc (50′) is clearly much bluer than the inner part due to the presence of young stars. Interior to the ring, some isolated OB associations located in the inner spiral arms are visible. Only the part of M31 for which the intensity in the B band is higher than 24.0 mag arcsec^{-2} is shown. Gray levels: <0.90, 0.90 to 1.03, 1.03 to 1.16, 1.16 to 1.29, 1.29 to 1.42, 1.42 to 1.55, 1.55 to 1.68, >1.68

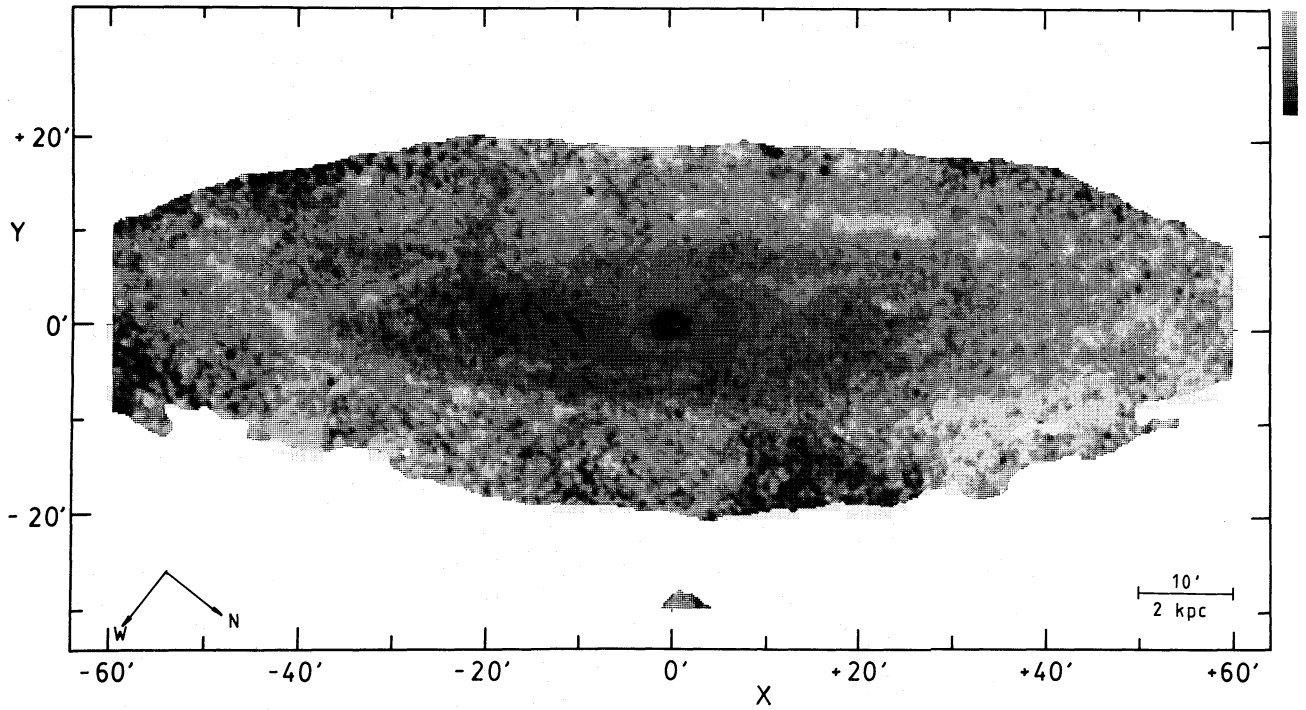

Fig. 5b. Map of the reddening free color index Q, defined according to the galactic reddening law as $(U-B)-0.72\,(B-V)$, at a resolution of 40″. Notice that dust lanes indeed are no longer visible. Some isolated OB associations appear in the inner spiral arm on the near side (bottom), which is very heavily reddened in the $U-V$ image. The calibration of the very central region (inner 5′) is not very reliable and the high Q color may not be real. Gray values (from light to dark): <-0.50, -0.50 to -0.43, -0.43 to -0.36, -0.36 to -0.29, -0.29 to -0.22, -0.22 to -0.15, >-0.15

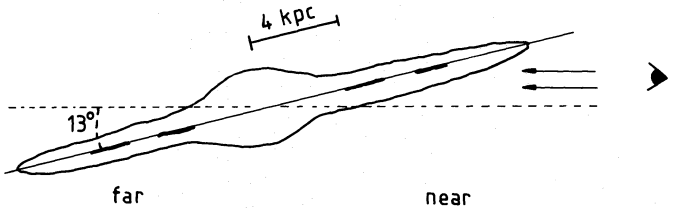

Fig. 6. Sketch of the location of an observer on the earth with respect to the disk of M31. Most of the bulge light and a major fraction of the disk light is behind the dust lanes on the near side due to the high inclination of the galaxy

For an infinitely thin thust layer the observed intensity is the sum from the contributions of unobscured light in front of the dust layer and obscured light behind the dust layer:

$$I_{\rm obs}(\lambda) = I_{\rm front}(\lambda) + I_{\rm back}(\lambda)\, e^{-\tau_\lambda} \tag{5a}$$

$$I_{\rm true}(\lambda) = I_{\rm front}(\lambda) + I_{\rm back}(\lambda); \tag{5b}$$

we assume $I_{\rm far} = I_{\rm true}$.

Let x be the fraction of light in front of the dust;

$$I_{\rm front} = x I_{\rm true}; \quad I_{\rm back} = (1-x)\, I_{\rm true}. \tag{6}$$

Then we can define:

$$I_\lambda \equiv \frac{I_{\rm obs}(\lambda)}{I_{\rm true}(\lambda)} = x + (1-x)\mathrm{e}^{-\tau_\lambda}. \tag{7}$$

The *observed* extinction in magnitudes in that case is [cf. (4)]:

$$A_\lambda = -2.5 \log (I_\lambda). \tag{8}$$

The optical depth values for different wavelengths are related according to the reddening law. For the galactic reddening law we have (Savage and Mathis, 1979):

$$\tau_U = 1.556\,\tau_V; \quad \tau_B = 1.323\,\tau_V; \quad \tau_R = 0.818\,\tau_V \tag{9}$$

leading to:

$$R_V = \frac{\tau_V}{\tau_B - \tau_V} = 3.1; \quad \frac{E(U-B)}{E(B-V)} = \frac{\tau_U - \tau_B}{\tau_B - \tau_V} = 0.72. \tag{10}$$

The *total, true* extinction in mag is proportional to the optical depth:

$$A_{\lambda,\,\rm tot} = 1.086\,\tau_\lambda. \tag{11}$$

The relation between the observed extinctions in two colors for different values of x as a function of τ_V is shown in Fig. 7. Only for $x = 0$ a linear relation holds. The maximum deviations from linearity occur for widely separated colors, so a comparison of A_U with A_R shows the effects best. The deviation is in the sense of relatively less reddening; for infinitely large optical depth and $x \neq 0$, the extinction observed in two color bands is the same, because only the light in front of the dust lane reaches the observer. Note that here the assumption is made that the fraction x is the same for all colors; this will be true on average if the scaleheight of the distribution of dust layers is smaller than the scaleheight of the star light in each color, a situation which is true to first order for such a highly inclined spiral, because most of the light behind and in front of the dust is relatively far away from the layer. In addition, we assume that the line of sight traverses only one dust layer. For multiple dust layers, the picture is qualitatively the same, but the exact relations are different. The distinction between one layer and multiple layers cannot be made from the data. The effect of clumping in the dust and the effects of light from behind the dust layer that is scattered into the line of sight of the observer, would also move the linear curve in Fig. 7 to the region occupied by curves for $x \neq 0$ (e.g. Caplan and Deharveng, 1986).

As an opposite example we consider a uniform, homogeneous layer of dust and stars, so in this case the dust layer has the same thickness as the stellar layer. Then the following well-known expression holds:

$$I_\lambda \equiv \frac{I_{\rm obs}(\lambda)}{I_{\rm true}(\lambda)} = \frac{1 - e^{-\tau_\lambda}}{\tau_\lambda}. \tag{12}$$

The resulting relation between A_U and A_R, again for a galactic reddening law, is also shown in Fig. 7.

Two important conclusions can be drawn from these geometrical considerations:

1. For small values of x (up to 0.2) and modest visual optical depths of the dust layer (up to 1.0, so a thin dust screen) the observed points in the diagram of A_U against A_R should lie close to the expected linear relation and the observed extinctions provide information on the reddening law.

2. The true optical depths may be significantly higher than indicated by the observed extinctions, even for small values of x; this is shown by the lines of constant optical depth in Fig. 7. An idea of the true extinctions can in principle be obtained from the positions of the observed points in the diagram (This is only true if one dust layer is present along the line of sight, and if light scattering and clumping are unimportant).

Another way to show the effects of a dust layer inside a stellar disk, is to plot the total extinction A_U against the selective extinction, $E(U-R)$; this diagram is shown in Fig. 12. It is similar to the "asymmetry curves" constructed by Elvius (1956) in a study of the dust lanes in several spirals. Again the curves demonstrate the important point that for dust mixed with star light, the reddening does not simply follow a Whitford curve, because the heavily reddened regions suffer so much extinction that they don't contribute much to the integrated colors of the galaxy.

5.1.2. Results

We obtained 8 scans in each color, passing through the nucleus and distributed around the minor axis with position angles in the plane of the sky ranging from 173° to 73°. Examples of scans can be found in Paper I (minor axis and West/East scan). The region between 0′ and 20′ from the nucleus was analyzed in steps of 30″. A 50″ aperture was used; this provided a reasonable compromise between spatial resolution and signal-to-noise. The diameter of the aperture corresponds to a linear distance of 167 pc, or 167 by 700 pc in the plane of the galaxy (on the minor axis). In addition, for the inner dust lane the signal-to-noise was sufficiently high that extinctions through a 16″ aperture could be measured as well. The apparent extinctions in all four color bands were derived for each scan according to expression (4). The resulting profiles of the extinction in B, A_B, for the 50″ aperture are shown in Fig. 8 (points), together with the integrated H I column densities in the disk, obtained through the same aperture (dashed curves).

The typical error in the derived extinctions due to photometric errors and plate noise is 0.05 to 0.1 mag for the inner region ($r < 10'$) and 0.1 to 0.2 mag for the outer region. Two major dust lanes can be identified in each scan; one corresponds to a spiral arm at about 4 kpc (5′ on the minor axis) from the nucleus, the other to an arm at about 9 kpc distance. The 4 kpc arm produces

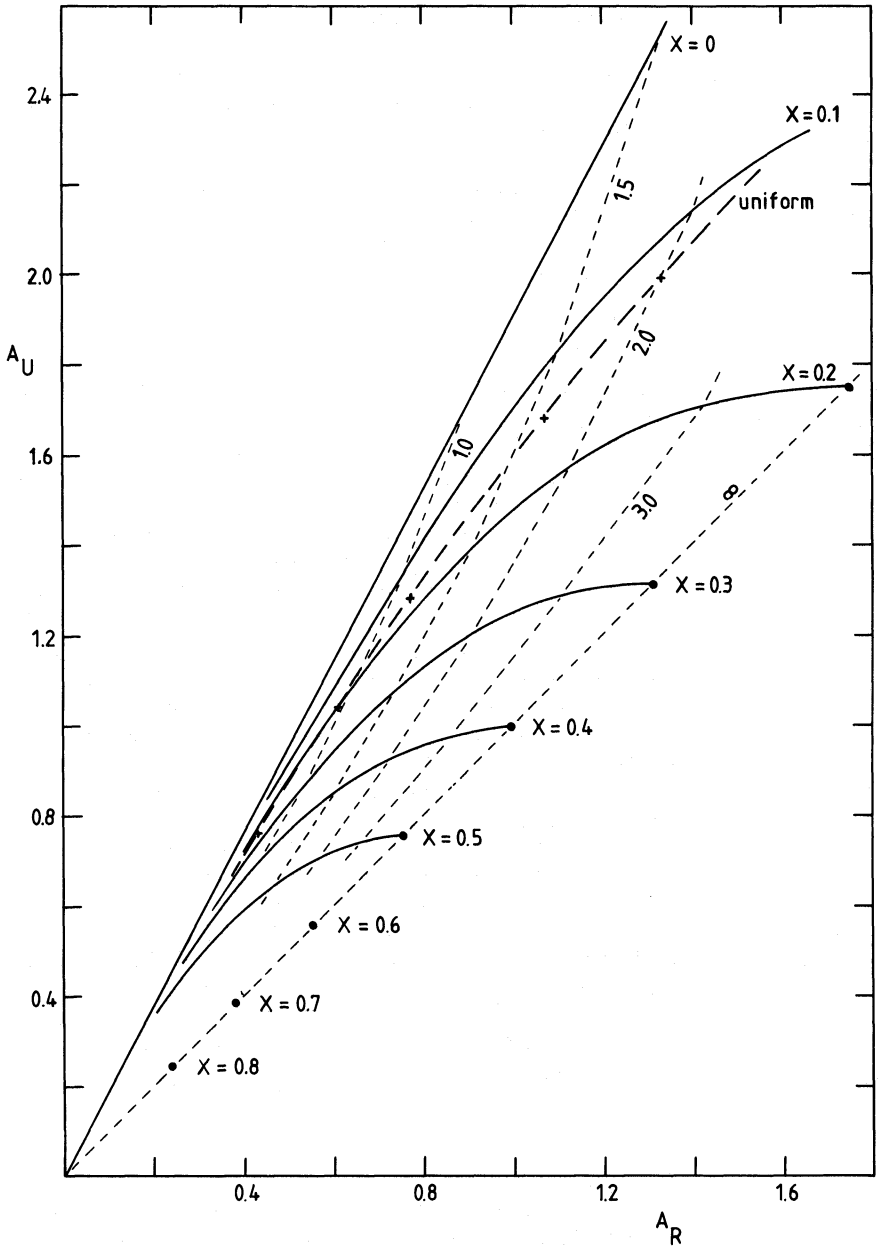

Fig. 7. The relation between the extinctions in U, A_U, and in R, A_R, that would be observed for an infinitely thin dust layer embedded in a stellar disk; the Galactic reddening law was assumed. x indicates the fraction of light that is in front of the dust layer. The parameter that varies along the curves is the true optical depth of the dust layer in the V band. The thin dashed lines connect points of equal optical depth. For infinite optical depth the observed extinctions in the two colors are the same because only the light that is in front of the dust reaches the observer. The long dashed line shows the expected relation for a uniform mixture of stars and dust. The plusses indicate the true optical depth of the dust layer for this case; values of 1, 1.5, 2, 3, and 4 are indicated

the most conspicuous dust lane in optical photographs. From H I and CO observations (Bajaja and Shane, 1982; Brinks, 1984; Stark, 1985) it is known that this arm has an apparent inward radial velocity of about 40 to 80 km s^{-1}. Only a few small OB associations and H II regions are present (Van den Bergh, 1964; Pellet et al., 1978; Fig. 5b) and it is basically a dust and gas arm. The 9 kpc arm is most obvious in H I and contains many star formation regions (Fig. 5a).

We derived the relations amongst the extinctions in the various color bands from the plots shown in Figs. 9–11. Figures 12 and 13 show diagrams of the total against selective extinctions for various color combinations. All measurements contaminated by foreground stars or OB associations on either the near or far side were deleted. Examples of such regions can be seen in the panels of Fig. 8, e.g. around $-15'$ in the scan with p.a. 98°, or around $-15'$ in the scan with p.a. 113°. Note that an association on the far side produces an apparent extinction on the near side.

Figures 9 and 10 show the results for the inner dust lane, for two different apertures. The relationships between extinctions in different color bands are essentially linear, consistent with the idea that all the light is behind the dust. The consistency between the relations derived for different apertures shows that clumping does not affect our results. The reddening law, derived from the *slopes* of the linear curves that were fit to the points in the diagrams, is listed in Table 2. The data are consistent with a reddening law equal to the Galactic law, although a somewhat lower value for R_V, 2.8, is indicated. Our value for R_V is in good agreement with the results from studies of globular clusters (Kron and Mayall, 1960; van den Bergh, 1969; Iye and Richter, 1985) that indicate values of 2.6. Hoessel and Melnick's results for the minor axis were also consistent with a normal Galactic value for R_V. Hodge and Kennicutt (1982) derived a somewhat higher value (4.3 ± 0.7), but this is based on a few data points. The scatter in our data is too large to put severe constraints on the ratio of $E(U-B)/E(B-V)$;

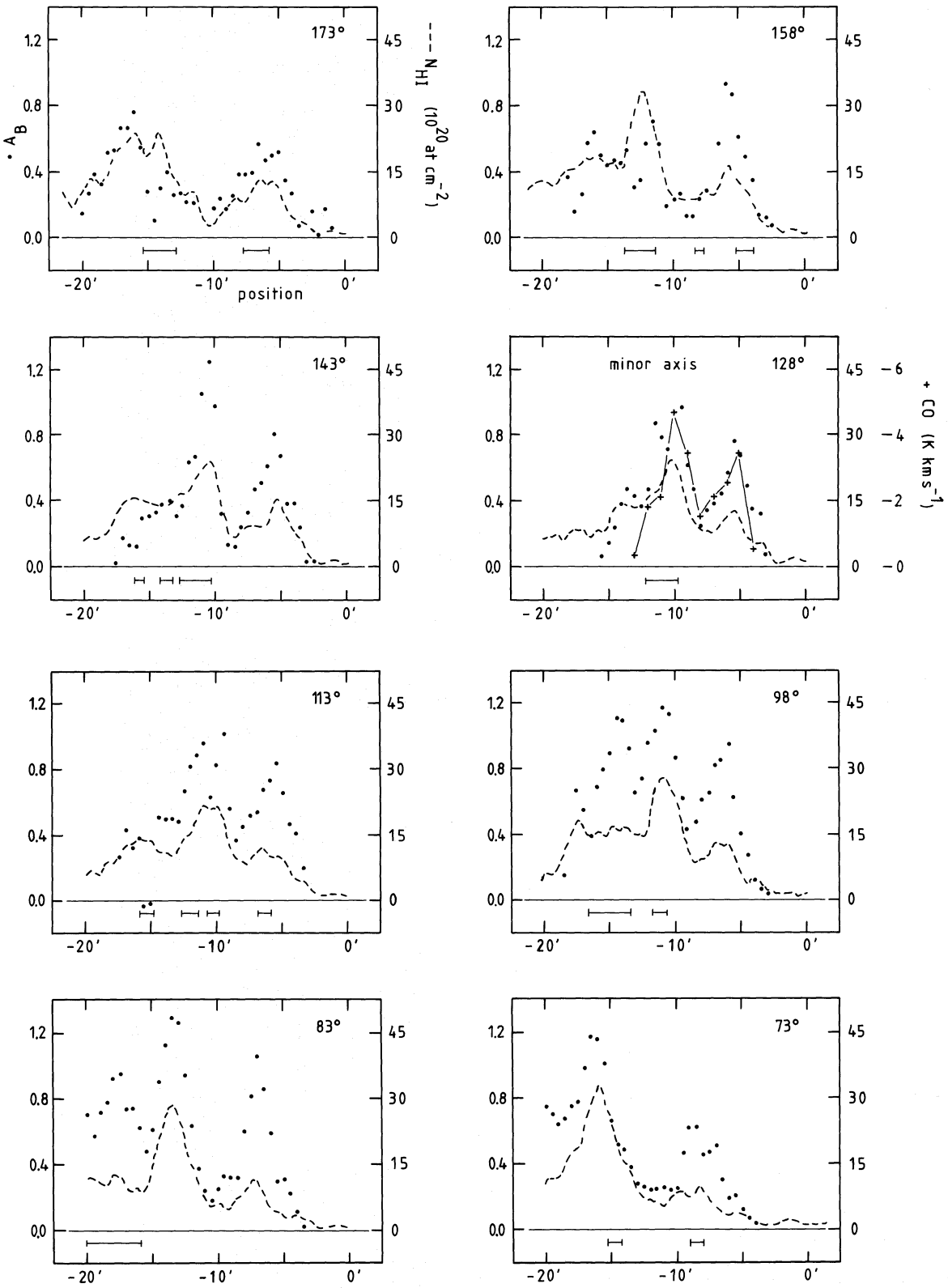

Fig. 8. The association between dust and H I gas in M 31 is illustrated in these panels, which show profiles of the extinctions in *B* on the near (West) side of the galaxy (dots) and of the column densities of neutral atomic hydrogen in the disk (dashed) for eight separate scans. An aperture of 50″ was used for both data sets. The position angles in the plane of the sky, measured from North to East, are indicated. The nucleus is located at position 0′. The bars below the cuts indicate regions where the derived extinctions are unreliable due to contamination by foreground stars or by OB associations on either the near of the far side of M 31. Notice that the observed extinctions may be lower limits to the true extinction (see text). For the minor axis cut, integrated CO antenna temperatures taken from Stark (1985) have been included as well. The H I column densities have been corrected for the contribution of gas associated with the warp (Brinks and Burton, 1984)

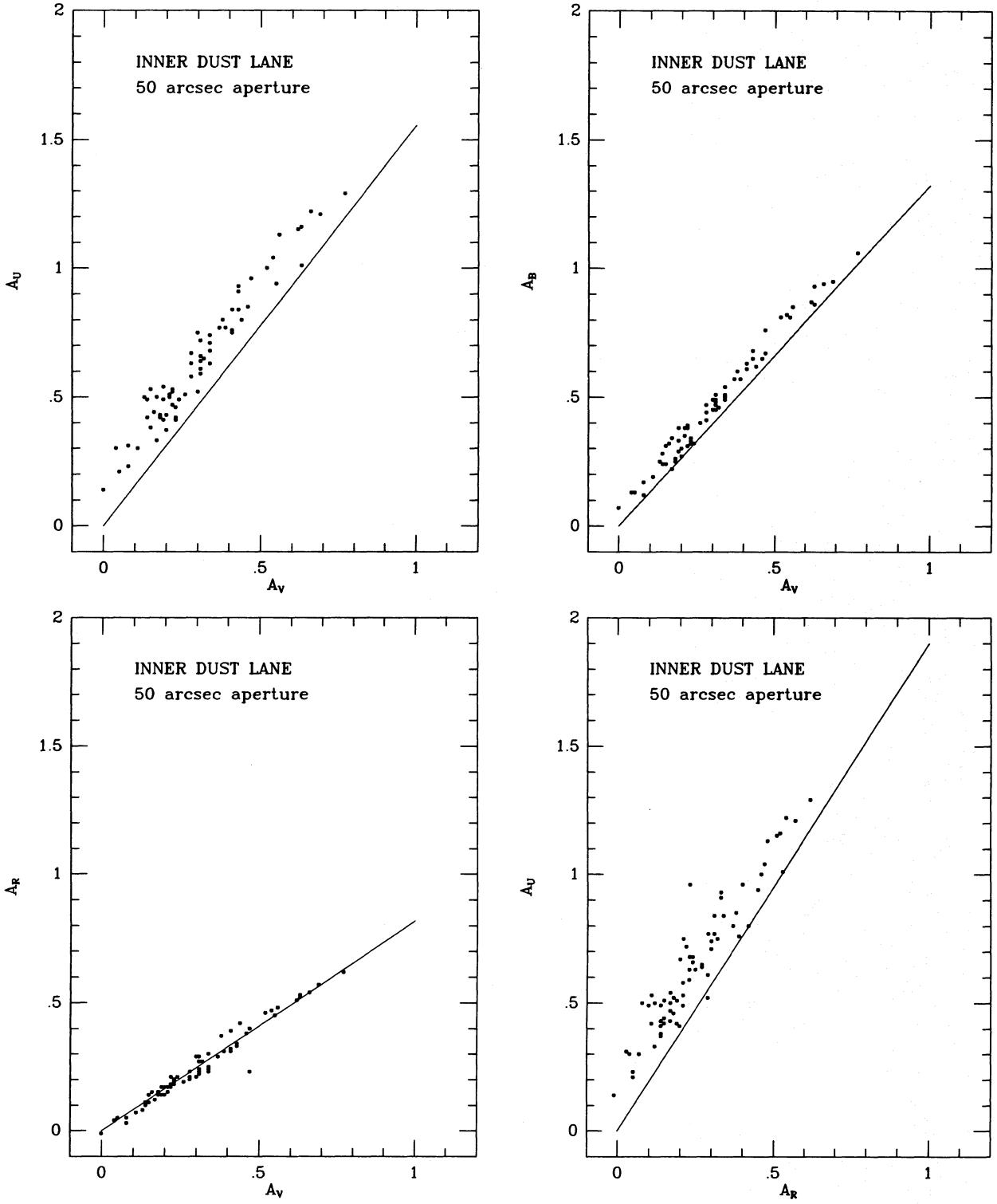

Fig. 9. The relation between the apparent extinctions in various colors that were derived from a comparison of the intensities measured through 50″ apertures on the near and far side of M31. The results of eight separate scans distributed around the minor axis are included. These panels show the results for a dust arm at roughly 4 kpc on the West side of M31. The lines show the relation expected from a Galactic reddening law with no foreground light towards the dust lane. Possible explanations for the systematic offset between the points and the line are discussed in the text. Typical measurement errors in the extinctions are $\leqq 0.1$ mag

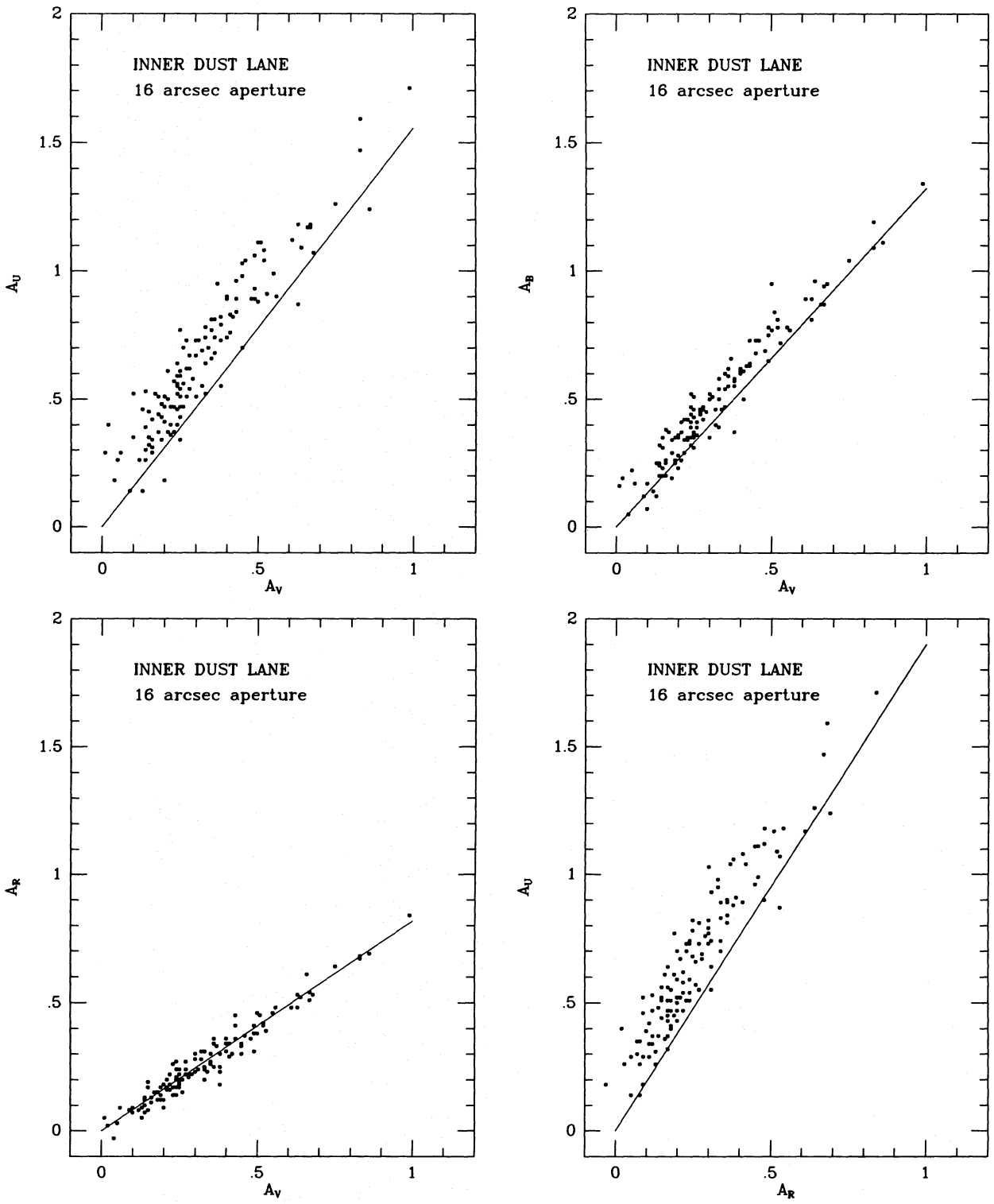

Fig. 10. Same as Fig. 9, but now for a 16″ aperture. The larger photometric errors in the small aperture result in more scatter than in Fig. 9

we cannot rule out the larger value (1.0) that was derived by Iye and Richter (1985) from a study of the globular clusters, but our data are more consistent with a lower value.

Figure 11 shows that the situation for the outer dust lane around 9 kpc is more complicated. The scatter in the derived extinctions is larger here than for the inner dust lane, because the photometric errors are larger at low intensities. Furthermore, the contamination by young stars in the disk of M31 is more severe. Linear fits to the points in these panels results in the relaticns listed in Table 2. Departures from the linear relation due to foreground light are suggested in the (A_U, A_R) plot. This is indicated by the curves corresponding to 10, 20, and 30% foreground light that are

Table 2. The reddening law in M31

Parameter	Inner lane	Outer lane[a]	Galactic law
A_U/A_V	1.53 ± 0.04	1.3 ± 0.1	1.556
A_B/A_V	1.35 ± 0.03	1.20 ± 0.08	1.323
$R_V = A_V/(A_B - A_V)$	2.8 ± 0.3	$3.5 - 7.0$	3.1
$E(U-B)/E(B-V)$	0.6 ± 0.2	–	0.72

[a] Outer lane possibly influenced by foreground light, see text (Sect. 5.1.2) for details

included in Fig. 11. However, much less evidence for this is found in the (A_U, A_V) plot and the direct comparison of A_V with A_R in Fig. 11 suggests that a systematic error in either V or R may be present. Such an error is not excluded by the uncertainties in the photometry at this brightness level. In any case, our data do not require a change in reddening law with distance, but the uncertainties are too large to be able to detect small differences.

Figure 12 shows the points for the two dust lanes in the A_U against $E(U-R)$ plot. It we assume that the R photometry is not affected by systematic errors, the lines of constant optical depth in this diagram suggest that the true optical depths in the dust lane around 9 kpc may reach a value of 2 to 2.5 (in a 50″ beam), which implies a maximum extinction in the V of about 2.2 or 2.7 mag. Hiromoto et al. (1983) found similar numbers from color variations in near-infrared scans. Elmegreen (1980) concluded that extinctions in prominent (face-on) dust lanes in spiral galaxies are also in this range.

A remarkable feature of the diagrams in Figs. 9 and 10 is the offset of the points for the inner dust lane with respect to the linear curve. The shift of the points means that there is a color difference between far and near side (the near side is too red or the far side too blue) that cannot be simply explained by reddening. The offset is in *opposite* sense to that expected from geometrical effects (Fig. 7) or clumping. The deviations are largest for the U band and decrease with increasing wavelength. The offsets cause a shift of the points to the botton right in the plots of total gainst selective extinction (Figs. 12 and 13a). For the outer dust lane the effect is smaller or absent. We have neglected the offsets in the derivation of the reddening law, which is based on the *slopes* of the fits to the points. Contrary to the offset between A_V and A_R in the outer dust lane, it is unlikely that the offsets for the inner dust lane are due to systematic errors in our analysis; errors in sky subtraction are unimportant at the levels we are dealing with here, and errors in the calibration curve of the photographic plates would affect both halves of the galaxy equally, Large scale asymmetries in the light of the galaxy would produce similar offsets for all colours, which is not observed; the same is true if an incorrect position for the nucleus would have been used in the comparison of near and far side intensities. Furthermore, de Vaucouleurs (1958) found similar departures in the plot of total against selective extinction for the minor axis of M31.

Offsets such as those discussed above have been noted for other spirals (e.g. Lindblad, 1941; Elvius, 1956) and more recently for the lenticular galaxy NGC 7070A (Brosch et al., 1985). The color dependence suggests that the effect may have to do with light scattering. Elvius (1956) analyzed several highly inclined spirals and extensively discussed the interpretation of the diagrams of total against selective extinction (her "asymmetry diagrams"). The diagrams for M31 are qualitatively similar to hers for NGC 4216; this was also noted by de Vaucouleurs (1958). According to Elvius (1956), points below the straight line in diagrams such as Fig. 12 can be explained by the effects of bulge light scattered off the disk in the direction of the observer. The major problem with this interpretation is, however, that in her picture the *bright* side of the galaxy is the near side. From studies of the reddening of globular clusters (Iye and Richter, 1985) it is known that this is definitely *not* the case for M31. The analysis by Elvius is based on the assumption that the scattered light would be relatively blue, i.e. scattering would be more color selective than absorption. On the other hand, observations of the Merope Reflection Nebula in the Milky Way (Andriesse et al., 1977) indicate that blue and ultraviolet light is scattered more or less isotropically and red light most strongly in forward direction. If that is the case, we would expect a relative increase of the intensity of red light on the near side. This would at least qualitatively be consistent with the observations: the extinctions in R are smaller than the extinctions in U predict (Fig. 9). In this respect it is interesting to note that the spectrum of light reflected off a high latitude cloud in the Milky Way (Mattila, 1979) is much redder than what would be expected from reflected light from the interstellar radiation field (de Vries, 1986).

There is in principle another effect that can introduce a shift of the points in the observed sense: the presence of dust on the far side. This dust will in general have a large amount of light in front of it. If, in addition, it has considerable optical depth, the far side of the galaxy will be somewhat obscured, but not much reddened. Because we subtract (in magnitudes) the near side from the far side, the obscuration on the far side results in reduced observed extinctions for the near side and, more important, the reduction would be relatively strongest for the extinction in R. The problem with this interpretation is that a large optical depth for the dust on tha far side would be required to account for the observed *relative* shift of about 0.15 mag in A_U compared to A_R (Fig. 9). From a diagram such as Fig. 7 we estimate that if 80% of the light is in front of the dust, τ_V would have to be at least 5 to produce the observed shift. Such dust lanes would produce observable extinctions of order 0.2 to 0.4 mag in all colors. In direct tracings of the light distribution on the far side no such dust lanes in the region of interest are found.

One last point that might be of relevance, concerns the assumption of constant x for all colors. If the scale height of the red light is higher than the scaleheight of the ultraviolet light, the observed extinctions in R would be systematically lower than those in U if the dust layer on the near side is displaced from the midplane in the direction of the observer, because in that case the fraction of light in front of the dust, x, would be larger in R than in

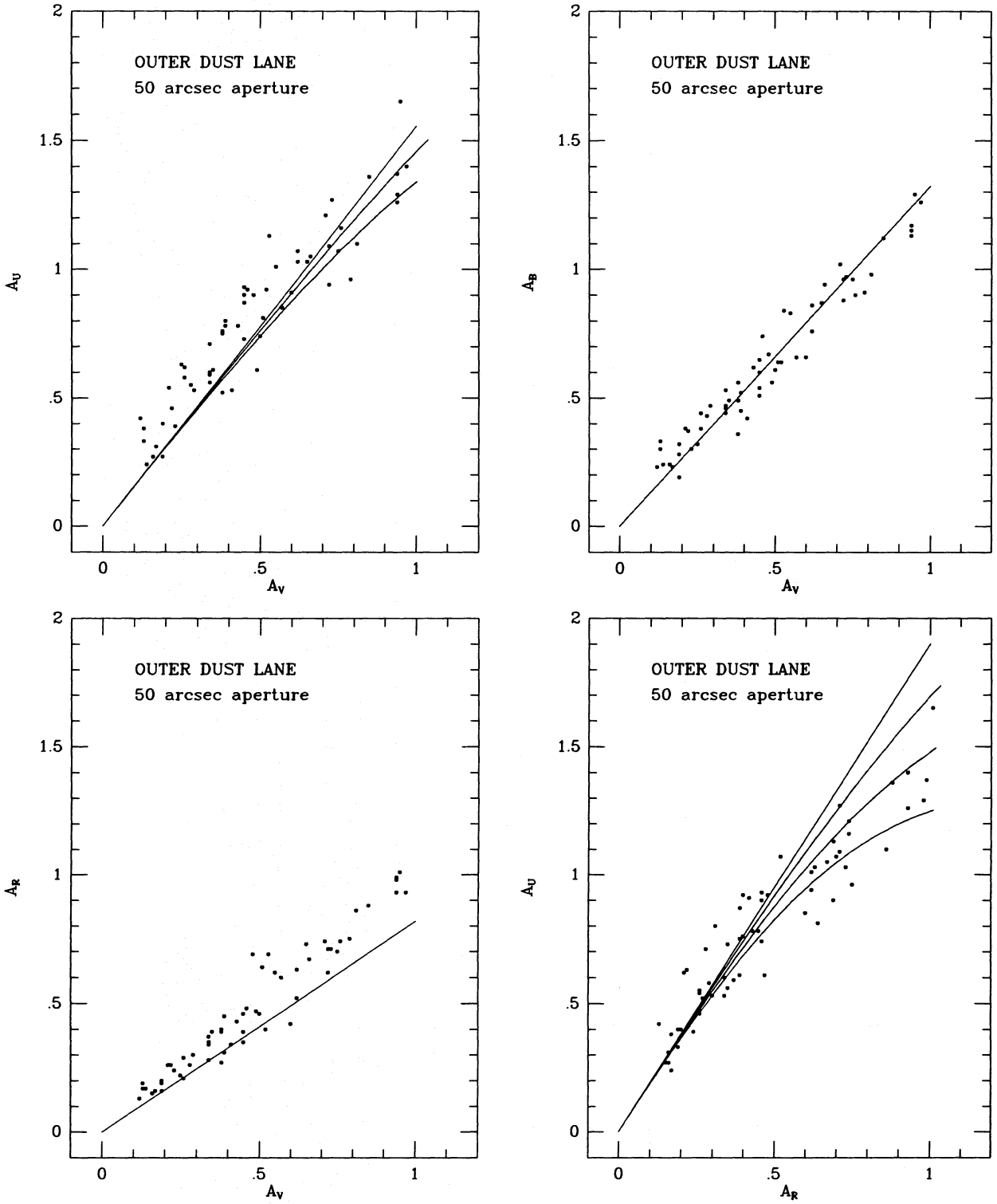

Fig. 11. Same as Fig. 9, but now for a dust lane at about 9 kpc from the center. The lines again show the relation predicted from a galactic reddening law. Two of the panels include lines which show the relations expected if some fraction of the light along the line of sight is in front of the dust; indicated are lines corresponding to fractions of 10 and 20% (and 30% for the bottom right panel) of foreground light (compare Fig. 7). The estimated errors in the individual points are $\leqq 0.2$ mag. The plot of A_U against A_R shows that foreground light may play a role in this lane, but this is not certain because the (A_R, A_V) diagram suggests that a systematic error is present in either A_V or A_R (compare with Fig. 9 or 10 where the photometric errors are smaller and no offset between A_V and A_R is present)

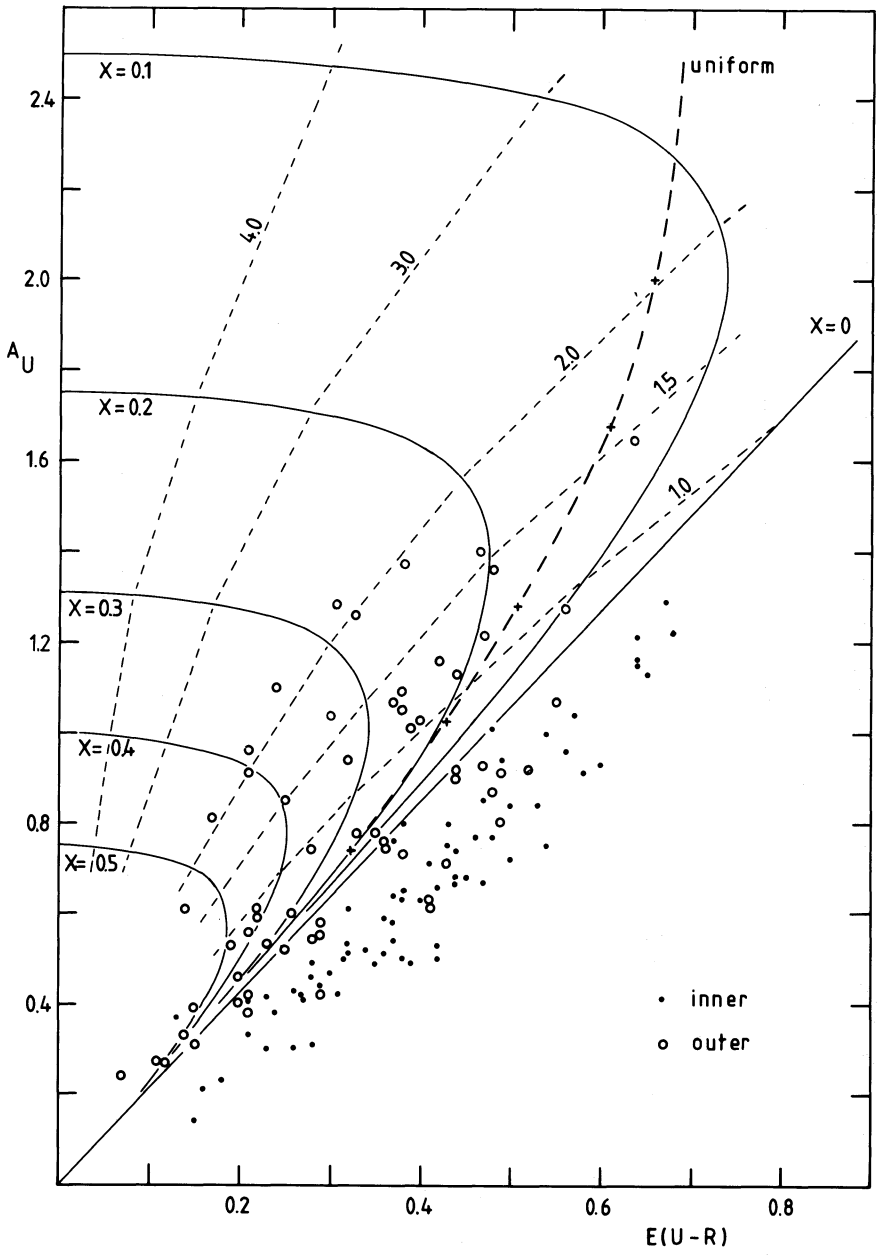

Fig. 12. A different way of showing the effects of foreground light on the measured extinctions is shown in this diagram of the relation between apparent extinctions in the U band and *selective* extinction. Points for the inner and outer dust lane (50″ aperture) are plotted. The expected relations for a thin dust layer embedded in a stellar disk are indicated by the thin drawn curves for various fractions, x, of the amount of light that is in front of the dust (the galactic reddening law was assumed). The case of a uniform mixture of dust and stars is indicated by the long dashed line. Values of constant visual optical depth of the dust layer are connected by the short dashed lines (cf. Fig. 7)

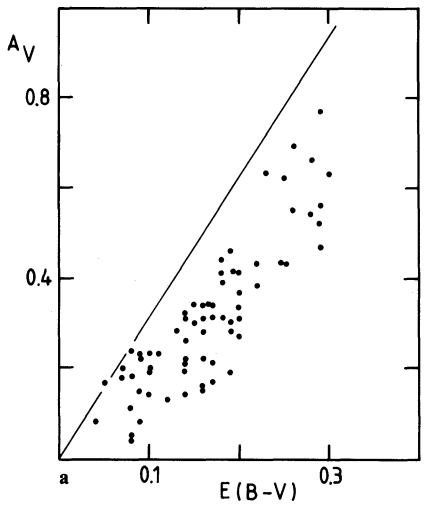

Fig. 13a. Same as Fig. 12 but now for the relation between A_V and $E(B-V)$ for the inner dust lane. The line indicates the expected relation for the galactic reddening law if all dust is in front of the light ($x=0$). The slope of the relation followed by the points is consistent with the galactic reddening law. The origin of the systematic shift between the points and the line is discussed in the text

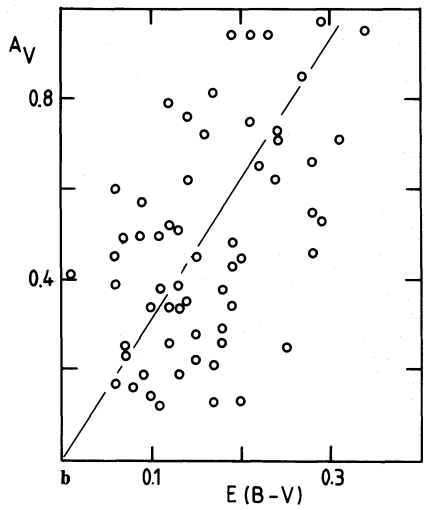

Fig. 13b. Same as Fig. 13a but now for the outer dust lane. The points seem to suggest a steeper slope than the galactic reddening law; this departure is in the sense expected if some light is in front of the dust

U. However, since most of the light in the region of the inner dust lane is contributed by the bulge a difference in scaleheight is not very likely.

To summarize, bulge light scattered off the dust in the disk is probably the cause of the offset. This explanation implies that red light is more strongly forward scattered than blue and UV light.

5.2. *The relation between gas and dust*

The close proximity of M31 allows a detailed quantitative comparison between dust and gas. Walterbos and Schwering (1987) studied the correlation between dust and atomic hydrogen gas, using the infrared emission as a tracer of the dust. The optical data, discussed in the previous section, provide new independent data on the dust and allow a comparison at much higher resolution, though limited to a smaller part of the galaxy.

The tight spatial correlation between dust and atomic gas in M31 has been noticed before (e.g. Unwin, 1980a, b; Brinks and Shane, 1984). Hodge (1980) found an apparent anti-correlation between dust and H I, but this was based on a comparison of the radial distributions of the number of dust clouds and the H I column density, and not of the actual amount of dust. The analysis of the infrared data (Walterbos and Schwering, 1987) shows evidence for a radial decrease in the dust-to-(atomic) hydrogen gas ratio, which might account for at least part of the result found by Hodge. The close spatial correlation between atomic gas and dust is well illustrated in the panels of Fig. 8 and on a more global scale in Fig. 14. The top picture shows a masked version of an optical map of M31 that was derived from a calibrated, digitized IIIaJ plate (Paper I). The map was obtained by dividing a high resolution intensity map by a smoothed version of the same map, but with foreground stars subtracted (see Paper I). The spatial filtering removes the large scale light distribution and enhances the contrast for small scale structures. The bottom half of the figure shows the full resolution ($23'' \times 35''$) integrated H I map from Brinks and Shane (1984), on the same grid as the dust map. We blinked the two maps and found that the correlation between dust and H I features is striking on all scales, down to the resolution limit of the H I data (roughly 100 pc). A rectified version of the masked image is shown in Fig. 15. It gives a good impression of the complicated spiral arm structure of M31; clearly, arm segments can be traced over distances of several tens of kpc, but no regular two or one armed pattern emerges, consistent with earlier findings.

The correspondence between dust and neutral atomic gas can be studied quantitatively by comparing the extinctions in the dust lanes that were derived in Sect. 5.1.2, with the corresponding H I column densities. Brinks and Burton (1984) derived a model for the H I warp of M31 and separated the gas in the disk from the gas in the warp. We used their maps to derive the H I column densities of the disk and the total H I column densities; the same aperture ($50''$) was used as in the optical measurements. The distinction between total H I and disk H I is important near the minor axis, because the gas layer in the outer parts is so severely warped that it is projected into the line of sight towards the disk on the near side M31. Figure 8 shows a direct comparison between the measured extinctions in the dust lanes and the disk H I column densities. The structure of the two components is very similar; the arm widths are the same and the positions of the peaks coincide.

For the minor axis, information on the molecular gas is available from CO data (Stark, 1985). The CO profile is similar to the dust and H I gas profiles. A conservative conversion factor of $2.5\ 10^{20}\,\mathrm{mol\,cm^{-2}}$ per integrated degree antenna temperature (Ryden and Stark, 1985) results in mass surface densities in the line of sight between 2.5–16.0 $M_\odot\,\mathrm{pc}^{-2}$, in the same range as the neutral gas surface densities (5–20 $M_\odot\,\mathrm{pc}^{-2}$) and not much less, as has been claimed before (e.g. Stark, 1985; cf. also Walterbos, 1986). Thus part of the extinction will be due to dust associated with molecular gas. However, for lack of more CO data we can only make a comparison of dust with H I data.

The relation between observed extinction and neutral gas column density in the two dust lanes is shown in Fig. 16. To assess the effects of gas associated with the warp, diagrams are shown for both the total H I column density and the disk H I column density. A linear relationship between A_B and $N_{\mathrm{H\,I}}$ is suggested by the figures. However, there is an offset in the sense that the extinction already drops to zero while a finite amount of H I is still indicated. It would be of interest for theories of grain formation if this would be a physical effect (no dust unless a certain amount of gas is present), but several other explanations can be thought of as well. One of these is that the observed extinctions might all have been underestimated by a more or less constant amount (0.1 to 0.2 mag) due to the fact that our assumption that the far side is not obscured is incorrect, or due to bulge light scattered into the line of sight. Such an underestimate could also result from light in front of the dust on the near side. Finally, the effect may indicate that the H I column densities are still contaminated by gas in the warp. A lower dust-to-gas ratio is indicated for the gas in the warp (see below), so this gas would not produce much extinction but it would contribute to the gas column density.

The panels in Fig. 16 show that the scatter is significantly smaller if disk H I column densities are used instead of total column densities, especially for the outer dust lane (correlation coefficients of 0.86 and 0.79). Because the extinctions that we have derived should be sensitive to all dust in front of the light, this implies that the warped gas apparently produces relatively less extinction, suggesting a lower dust-to-(atomic) hydrogen gas ratio there. A more detailed picture of the variation of this ratio may be obtained from Fig. 17, where we plot the ratio of A_B to $N_{\mathrm{H\,I}}$ as a function of distance to the center. The positions on the profiles were converted to a position in the plane of the galaxy, assuming an infinitely thin dust and H I gas layer and an inclination of 77°. The observed extinctions and disk H I column densities were used, and no correction was applied for the offset in $N_{\mathrm{H\,I}}$ for zero extinction than is seen in Fig. 16. Correcting for this offset, by subtracting it from the H I column densities before the division, would result in a slightly steeper radial dependence than is now found in Fig. 17. The value predicted for the dust-to-(atomic) hydrogen gas ratio observed in the solar neighborhood (Savage and Mathis, 1979) is indicated. This value is based on total extinction along the line of sight, so it includes dust in *molecular* clouds, which is also the case in our comparison.

The interpretation of Fig. 17 is hampered by the fact that in principle all observed extinctions may be lower limits to the true extinction. In particular, the departures from the expected linear relation in Fig. 11 indicate that this is almost certainly true for the outer dust lane around 9 kpc, although as discussed in Sect. 5.1.2, systematic errors in the photometry may play a role as well.

In spite of these limitations some important conclusions can be drawn from our analysis:

1. The observed extinctions have values that are compatible with a dust-to-gas ratio equal to that in the solar neighborhood.

2. A possible radial variation in dust-to-(atomic) hydrogen gas ratio is probably flatter than indicated by the points in Fig. 17, because it is unlikely that the extinctions in the inner dust lane would be more underestimated than the extinctions in the outer

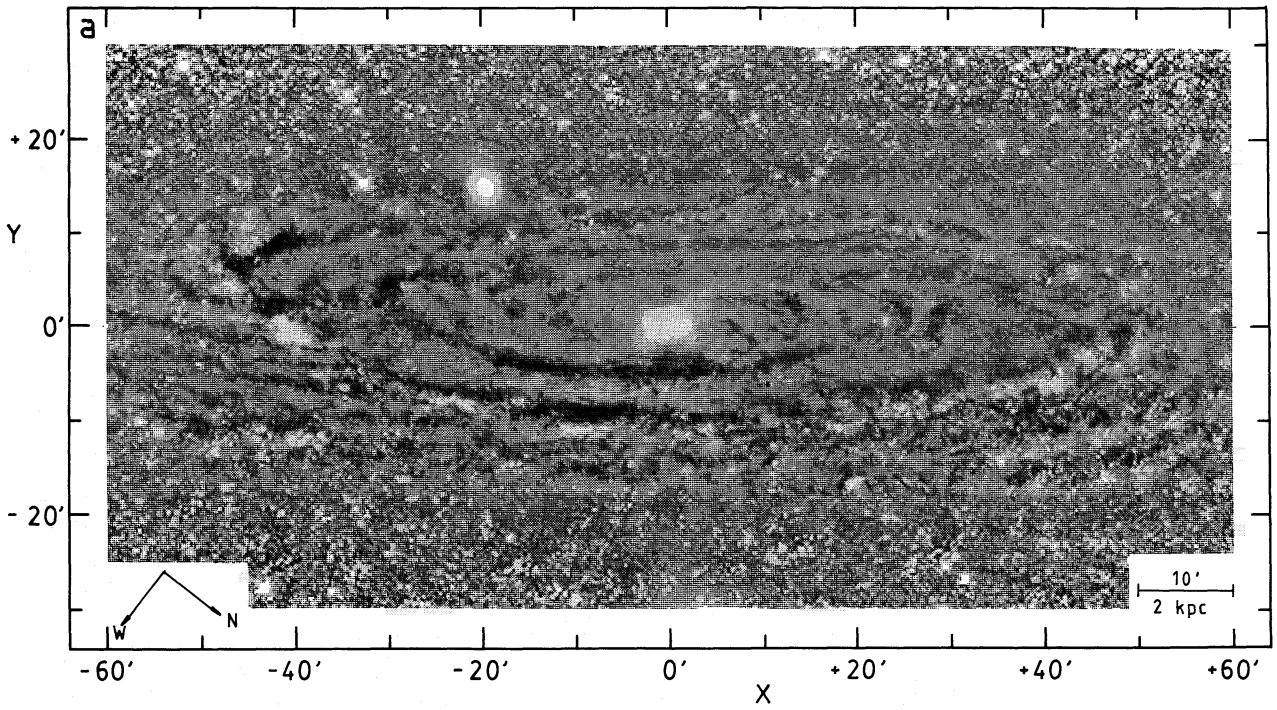

Fig. 14a. Masked image obtained from calibrated IIIaJ plates. The masking removes large scale light gradients and highlights structural features in the light distribution such as dust lanes (dark) and bright associations (light). Structures larger than 5′ are attenuated by the filtering process. At least four spiral arm crossings can be seen on the near side of M 31 (bottom side in figure). The light of the bulge of M 31 and of the elliptical M 32 is not removed by the filtering, because the intensity gradients are too steep

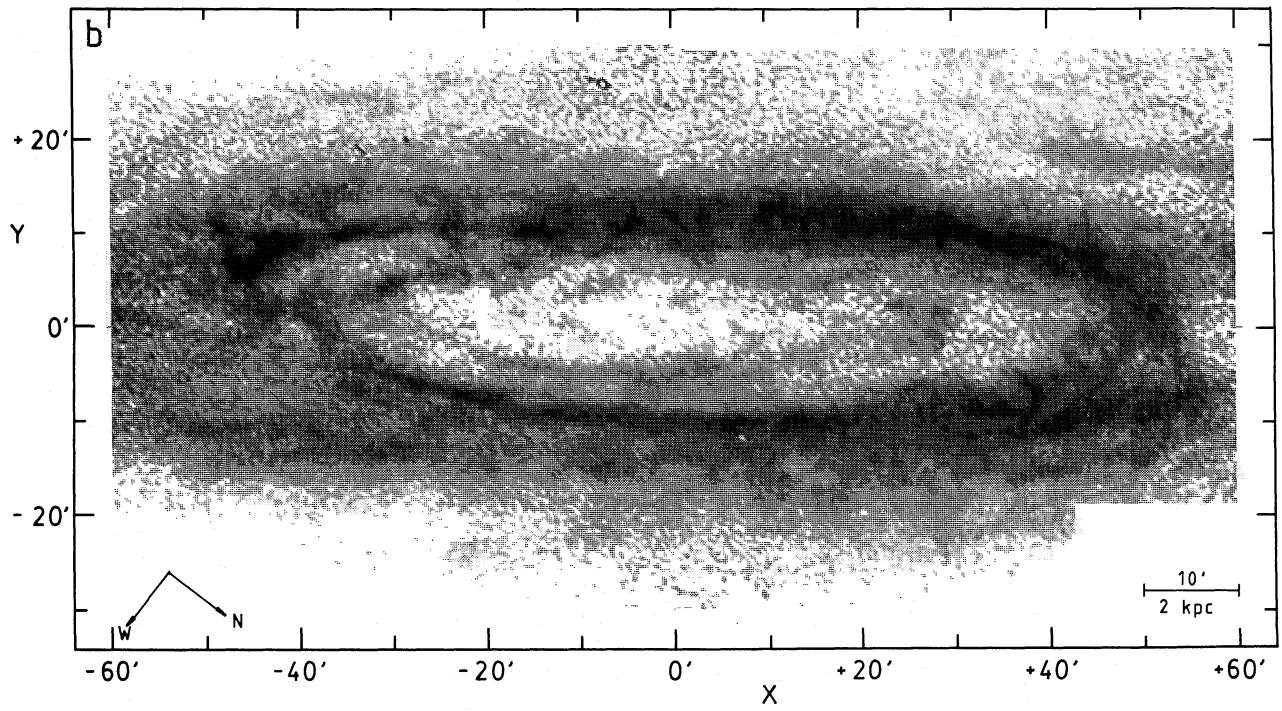

Fig. 14b. The integrated H I map from Brinks and Shane (1984) on the same scale as the dust map above. Notice the striking correlation between H I and dust, on all scales down to the resolution limit. A nice example are the dust clouds on the major axis around $X = +28'$

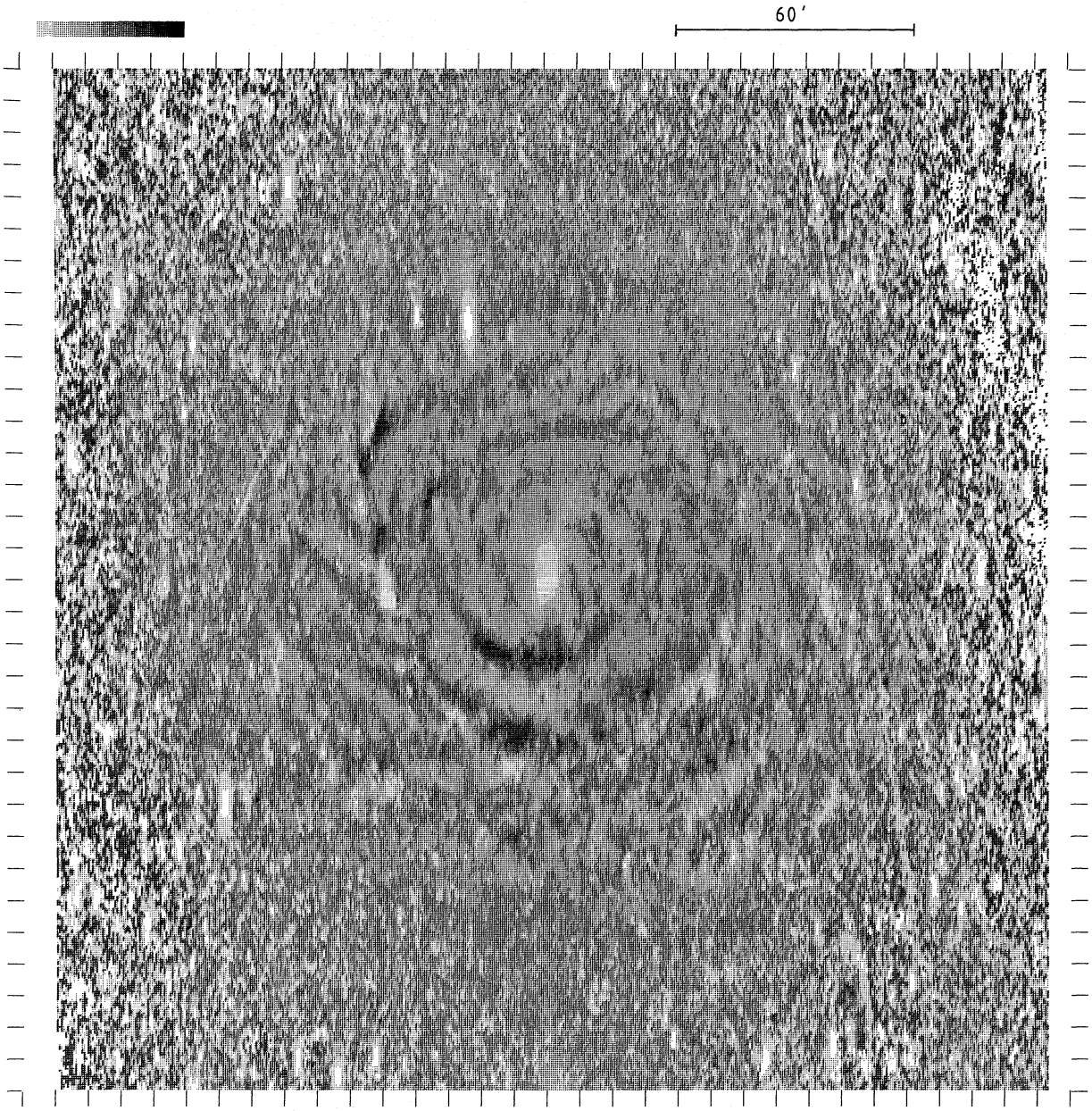

Fig. 15. The image of Fig. 14a, regridded to a face-on projection, for an inclination of 77°. Long spiral arm filaments can be clearly traced, but no regular two or one armed spiral is discernible

dust lane (cf. Figs. 9 and 11). The maximum gradient indicated by these points corresponds to an exponential scalelength of about 8 kpc. The optical data certainly do not rule out a radial dependence of the dust-to-gas ratio; especially the indications for the low dust content in the warped H I gas are consistent with a radial variation. The scalelength of the metal-abundance gradient, roughly 12 kpc (Blair et al., 1982) is also compatible with the upper limit on the variation in dust-to-gas ratio. It should be pointed out, however, that a radial variation in dust-to-(atomic) hydrogen gas ratio found from an analysis as this one could also be caused by a radial variation of the N_{H_2} to N_{HI} ratio, because the extinctions are sensitive to all dust. The scatter in Fig. 16 is probably also at least in part due to the neglect of the molecular gas.

Bajaja and Gergeley (1977) compared the reddening of globular clusters with the H I column densities along the line of sight and found a decrease of about a factor of 1.5 to 2 in the dust-to-(atomic) hydrogen gas ratio between 5 and 12 kpc. A study of the radial variation of the dust-to-(atomic) hydrogen gas ratio based on an analysis of the infrared emission from the dust in M 31 (Walterbos and Schwering, 1987), indicates a steep gradient (scalelength of about 4 kpc), but that analysis is complicated by possible effects of small grains on the infrared emission. The conclusion of that paper is that a real gradient is present, but with a larger scalelength than 4 kpc. Unfortunately, a direct comparison with the infrared results is difficult, because the resolution of the IRAS data is much lower. For the outer dust lane, the extinctions indicated by the cool dust map (see Walterbos and Schwering, 1987) are higher than the optical values derived above by a factor varying between 1 to 2.5, not inconsistent with the present results. The inner dust lane is not well separated from the

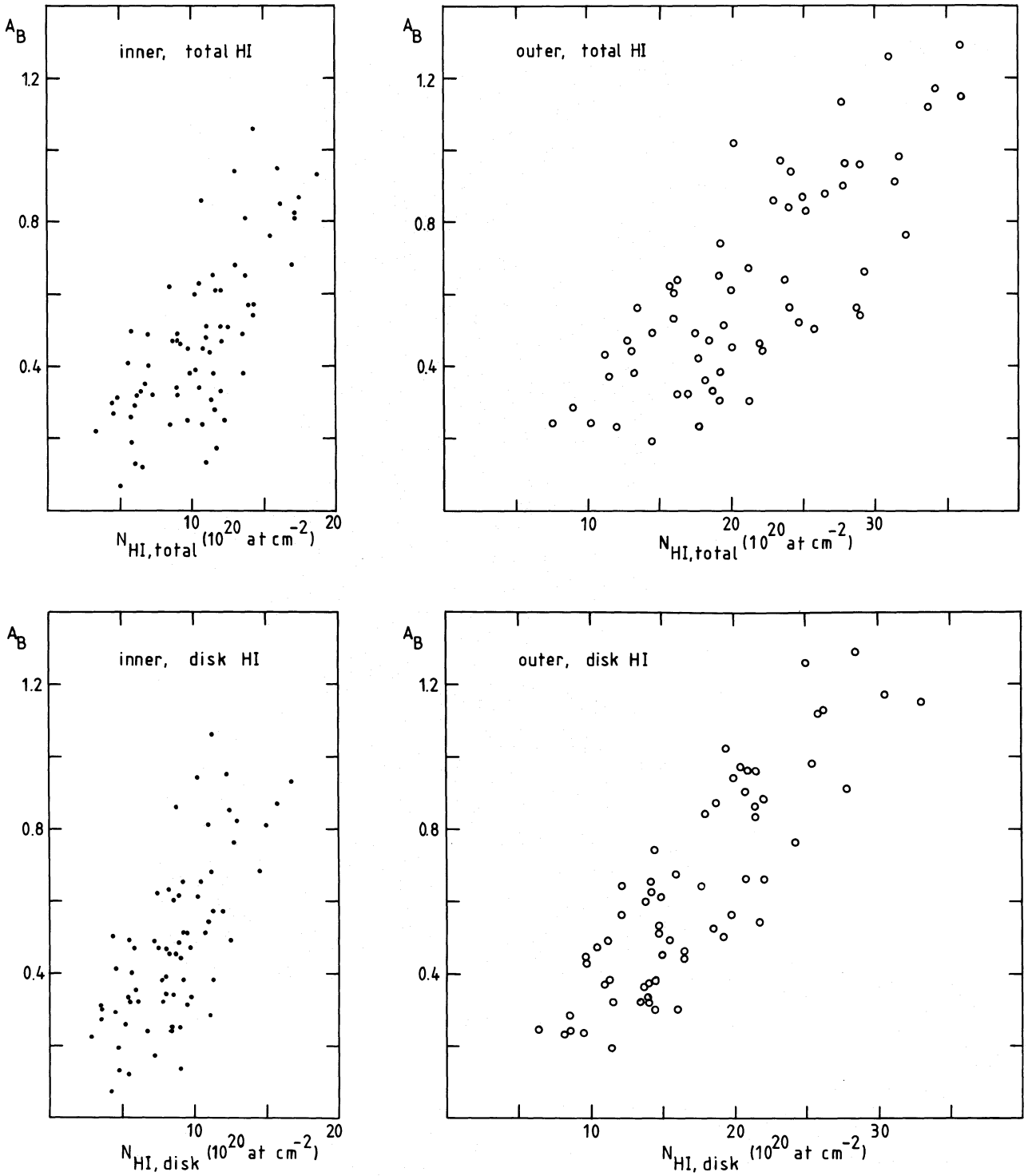

Fig. 16. Diagrams showing the relation between the observed extinction in the *B* band and H I column density. The results for the inner (4 kpc) and outer (9 kpc) dust lane are shown separately. If only the disk H I column density is used (bottom figures), the scatter is reduced. The extinctions may be lower limits to the true extinctions (see text)

nuclear emission in the IRAS data and a comparison with the optical data is not possible here. A further complication is the fact that the IRAS data are mainly sampling dust associated with diffuse H I gas, while the optical extinctions are sensitive to both dust in H I and dust in H_2 clouds.

6. Summary of results

The main results of our study of stars and dust in M31 are as follows:

1. The position angle of the outer parts of the disk changes significantly for radii larger than 90′ (18 kpc), in agreement with

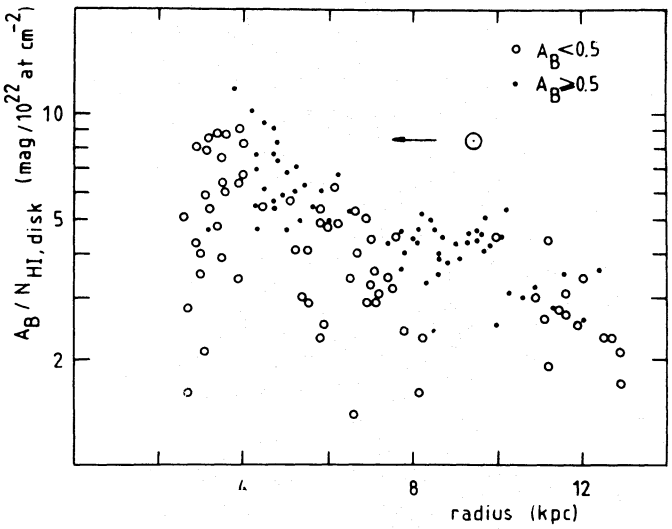

Fig. 17. The ratio of the extinction in B to the H I column density in the disk as a function of distance to the center. The points with low extinction generally fall below the other points as a result of the finite amount of H I for zero extinction (cf. Fig. 16), for which no correction was applied here. The value expected for a dust-to-(atomic) hydrogen gas ratio similar to that in the solar neighborhood is indicated. The interpretation of this diagram is complicated by the fact that all extinctions may be lower limits to the true extinction (see text)

earlier findings (Innanen et al., 1982). On the SW side the change seems to indicate a warping of the stellar disk; for the NE side the results are less conclusive, because the emission is very faint there.

2. The intensity and color profiles along the two main axes were decomposed in bulge and disk components (see Table 1). It is shown that the earlier classification of the disk profile of M31 as "type II' is most likely due to the influence of spiral arms.

3. The bulge profile can be well represented by an $r^{1/4}$ law. The bulge contributes roughly 40% of the observed total light. There is no evidence for a radial color gradient in the bulge.

4. An exponential fit to those parts of the disk that do not seem to be influenced by spiral arms, indicates that the colors of the disk get bluer with increasing distance to the center. The color gradient is about 0.02 mag kpc^{-1} in $B-R$. The inner part of the disk has colors typical of an old, metal rich stellar population. The color variation may be due a variation in metal abundance, but age effects may also contribute.

5. The analysis of the two major dust lanes on the near side of M31 shows that the extinction law in M31 is very similar to that in the Galaxy. A value of 2.8 ± 0.3 is derived for the ratio of total to selective extinction in the visual. Diagrams of the observed extinction in one color against that in another color show systematic offsets with respect to the expected relation; similar offsets are observed in other spirals. The offsets are in the sense that the near side of the galaxy is relatively red. They can probably be explained by scattering of bulge light off the dust in the disk. If this explanation is correct, the observations imply that red light is scattered more strongly in forward direction than blue and ultraviolet light.

6. A striking correlation between dust and atomic hydrogen gas is indicated by comparison of a masked optical image and a high resolution map of the H I distribution. The correlation is studied quantitatively by a point-to-point comparison of dust and gas in the two major dust lanes on the near side. The resulting dust-to-(atomic) hydrogen gas ratios are consistent with the value for the solar neighborhood, but do not rule out a radial decrease of this ratio. In particular, the dust content of the gas in the warp seems to be low.

Acknowledgements. We thank Drs. G. de Vaucouleurs, F.P. Israel, and J.M. van der Hulst for useful discussions. R.A.M. Walterbos was supported by the Netherlands Foundation for Astronomical Research (ASTRON) with financial aid from the Netherlands Organization for the Advancement of Pure Research (ZWO), and by NASA grant NAS 8-32902. R.C. Kennicutt was suported by NSF Grants AST 81-11711 A01 and 86-13257 and an Alfred P. Sloan Fellowship.

References

Andriesse, C.D., Piersma, Th.R., Witt, A.N.: 1977, *Astron. Astrophys.* **54**, 841
Baade, W.: 1963, in *Evolution of Stars and Galaxies*, Harvard University, Cambridge, Massachusetts, p. 73
Baade, W., Arp, H.: 1964, *Astrophys. J.* **139**, 1027
Bajaja, E., Gergeley, T.E.: 1977, *Astron. Astrophys.* **61**, 229
Bajaja, E., Shane, W.W.: 1982, *Astron. Astrophys. Suppl.* **49**, 745
Blair, W.P., Kirshner, R.P., Chevalier, R.A.: 1982, *Astrophys. J.* **254**, 50
Boroson, T.: 1981, *Astrophys. J. Suppl.* **46**, 177
Brinks, E.: 1984, Ph. D. thesis, University of Leiden
Brinks, E., Burton, W.B.: 1984, *Astron. Astrophys.* **141**, 195
Brinks, E., Shane, W.W.: 1984, *Astron. Astrophys. Suppl.* **55**, 179
Brosch, N., Greenberg, J.M., Grosbol, P.J.: 1985, *Astron. Astrophys.* **143**, 399
Caplan, J., Deharveng, L.: 1986, *Astron. Astrophys.* **155**, 297
Ciardullo, R., Ford, H.C., Neill, J.D., Jacoby, G.H., Shafter, A.W.: 1987, *Astrophys. J.* **318**, 520
Cram, T.R., Roberts, M.S., Whitehurst, R.N.: 1980, *Astron. Astrophys. Suppl.* **40**, 215
de Vaucouleurs, G.: 1948, *Ann. d'Astrophys.* **11**, 247
de Vaucouleurs, G.: 1958, *Astrophys. J.* **128**, 465
de Vries, C.P., Le Poole, R.S.: 1985, *Astron. Astrophys. Letters* **145**, L7
de Vries, C.P.: 1986, Ph. D. thesis, University of Leiden
Elmegreen, D.M.: 1980, *Astrophys. J. Suppl.* **43**, 37
Elson, R.A.W., Walterbos, R.A.M.: 1988, *Astrophys. J.* (in press)
Elvius, A.: 1956, *Stockholm Obs. Ann.* **18**, No. 9
Freeman, K.C.: 1970, *Astrophys. J.* **160**, 811
Gallagher, J.S., Hunter, D.A.: 1981, *Astron. J.* **86**, 1312
Henderson, A.P.: 1979, *Astron. Astrophys.* **75**, 311
Hiromoto, N., Maihara, T., Oda, N.: 1983, *Publ. Astron. Soc. Japan* **35**, 413
Hodge, P.W.: 1980, *Astron. J.* **85**, 376
Hodge, P.W., Kennicutt, R.C.: 1982, *Astron. J.* **87**, 264
Hoessel, J., Melnick, J.: 1980, *Astron. Astrophys.* **84**, 317
Innanen, K.A., Kamper, K.W., Papp, K.A., van den Bergh, S.: 1982, *Astrophys. J.* **254**, 515
Iye, M., Richter, O.-G.: 1985, *Astron. Astrophys.* **144**, 471
Jensen, E.B., Talbot, R.J., Dufour, R.J.: 1981, *Astrophys. J.* **243**, 716
Jensen, E.B., Thuan, T.X.: 1982, *Astrophys. J. Suppl.* **50**, 421
Kennicutt, R.C., Edgar, B.K.: 1986, *Astrophys. J.* **300**, 132
Kent, S.M.: 1983, *Astrophys. J.* **266**, 562
Kent, S.M.: 1985, *Astrophys. J. Suppl.* **59**, 115
Kron, G.E., Mayall, N.U.: 1960, *Astron. J.* **65**, 581

Lindblad, B.: 1941, *Stockholm Obs. Ann.* **13**, No. 8
Lindblad, B.: 1956, *Stockholm Obs. Ann.* **19**, No. 2
Low, F.I., Beintema, D.A., Gautier, T.N., Gillett, F.C., Beichman, C.A., Neugebauer, G., Young, E., Aumann, H.H., Boggess, N., Emerson, J.P., Habing, H.J., Hauser, M.G., Houck, J.R., Rowan-Robinson, M., Soifer, B.T., Walker, R.G., Wesselius, P.R.: 1984, *Astrophys. J. Letters* **278**, L19
Mattila, K.: 1979, *Astron. Astrophys.* **78**, 253
Newton, K., Emerson, D.T.: 1977, *Monthly Notices Roy. Astron. Soc.* **181**, 573
Pellet, A., Astier, N., Viale, A., Courtès, G., Maucherat, A., Monnet, G., Simien, F.: 1978, *Astron. Astrophys. Suppl.* **31**, 439
Price, J.S., Grasdalen, G.L.: 1983, *Astrophys. J.* **275**, 559
Ryden, B.S., Stark, A.: 1986, *Astrophys. J.* **305**, 823
Savage, B.D., Mathis, J.S.: 1979, *Ann. Rev. Astron. Astrophys.* **17**, 73
Schweizer, F.: 1976, *Astrophys. J. Suppl.* **31**, 313
Stark, A.: 1985, in *The Milky Way Galaxy, IAU Symp.* **106**, eds. H. van Woerden, R.J. Allen, W.B. Burton, Reidel, Dordrecht, p. 445
Tinsley, B.M.: 1980, *Fund. Cosmic Physics* **5**, 287
Talbot, R.J., Jensen, E.B., Dufour, R.J.: 1979, *Astrophys. J.* **229**, 91
Unwin, S.C.: 1980a, *Monthly Notices Roy. Astron. Soc.* **190**, 551
Unwin, S.C.: 1980b, *Monthly Notices Roy. Astron. Soc.* **192**, 243
van den Bergh, S.: 1964, *Astrophys. J. Suppl.* **9**, 65
van den Bergh, S.: 1969, *Astrophys. J. Suppl.* **19**, 145
van der Kruit, P.C.: 1979, *Astron. Astrophys. Suppl.* **38**, 15
van der Kruit, P.C.: 1984, *Astron. Astrophys.* **140**, 470
van der Kruit, P.C., Searle, L.: 1981, *Astron. Astrophys.* **95**, 105
van der Kruit, P.C., Searle, L.: 1982a, *Astron. Astrophys.* **110**, 61
van der Kruit, P.C., Searle, L.: 1982b, *Astron. Astrophys.* **110**, 79
van Genderen, A.M.: 1969, *Bull. Astron. Inst. Neth. Suppl.* **3**, 299
van Genderen, A.M.: 1973, *Astron. Astrophys.* **24**, 47
van Houten, C.J.: 1961, *Bull. Astron. Inst. Neth.* **16**, 1
Walterbos, R.A.M.: 1986, Ph. D. thesis, University of Leiden
Walterbos, R.A.M., Kennicutt, R.C.: 1987, *Astron. Astrophys. Suppl.* **69**, 311 (Paper I)
Walterbos, R.A.M., Schwering, P.B.W.: 1987, *Astron. Astrophys.* **180**, 27
Wevers, B.M.H.R.: 1984, Ph. D. thesis, University of Groningen
Wevers, B.M.H.R., van der Kruit, P.C., Allen, R.J.: 1986, *Astron. Astrophys. Suppl.* **66**, 505